NTNU – Trondheim
Norwegian University of
Science and Technology

Catalytic combustion control

Carina Renée Strand

Chemical Engineering and Biotechnology
Submission date: December 2012
Supervisor: Sigurd Skogestad, IKP
Co-supervisor: Johannes Jäschke, IKP
Krister Forsman, Perstorp

Norwegian University of Science and Technology
Department of Chemical Engineering

Catalytic combustion control

Carina Renée Strand

December 17, 2012

Preface

This thesis was written as the final part of my M.Sc degree in Chemical Engineering at the Norwegian University of Science and Technology.

I would like to thank all my three supervisors, Professor Sigurd Skogestad, Postdoc Johannes Jäsckhe, and Krister Forsman from Perstorp, for their invaluable help and endless support and encouragement throughout the whole period of writing this thesis. I am deeply grateful to all of you, and I am sure what I've learned through this thesis will benefit me greatly in my coming years as a researcher.

Declaration of Compliance

I, Carina Renée Strand, hereby declare that this is an independent work according to the exam regulations of the Norwegian University of Science and Technology.

Trondheim, December 17th 2012

Carina Renée Strand

Abstract

A mathematical model representing the dynamic behaviour observed at the actual catalytic incineration plant at Perstorp was derived. The model equations for the two main process units, the heat exchanger and the incinerator, were based on the lumped systems approach in order to avoid using partial differential equations. The model was written in Matlab and implemented in Simulink using s-functions for the dynamic study.

By analyzing the dynamic data from the actual plant, it was discovered that the possible source of the ocassional large temperature variations in the incinerator is the periodic variations in the inlet compositions, amplified the overly agressive air valve controller combined with a significant dead time. This results in oscillations due to overshooting. This behaviour was successfully reproduced using the derived model.

Two possibilities for improving the control performance were investigated, both using already existing sensors and actuators.

The first control improvement involved reducing the proportional gain according to the SIMC tuning rules for PI controllers. This resulted in a significant reduction in the amplitude of the oscillations in the temperatures throughout the reactor, and thus a more stable performance.

Finally, cascade control was implemented using the faster-responding catalyst bed temperature for the inner loop, and the reactor outlet temperature for the outer loop. This provided the most optimal results with the best disturbance rejection as it is able to compensate for the disturbance before it is detected in the outlet temperature.

Sammendrag

En matematisk modell som beskriver den dynamiske oppførselen observert ved det katalytiske insineratoranlegget ved Perstorp ble utledet. Modellikningene for de to hovedprosessenhetene, altså varmeveksleren og insineratoren, ble basert på lumped systems-metoden for å unng bruk av partielle differensiallikninger. Modellen ble skrevet i Matlab og implementert i Simulink ved hjelp av s-funksjoner for det dynamiske studiet.

Ved å analysere dynamiske datalogger fra det reelle anlegget ble det oppdaget en mulig årsak til de noen ganger signifikante temperaturvariasjonene i insineratoren – periodiske svingninger gasskomposisjonen, forsterket av en overagressiv regulator med betydelig dødtid. Dette førte til stadige oscillasjoner grunnet overshooting. Denne dynamiske oppførselen ble reprodusert ved bruk av modellen.

To muligheter for å forbedre prosessreguleringa ble undersøkt. Begge disse mulighetene brukte allerede eksisterende sensorer og aktuatorer i anlegget.

Den første forbedringsmetoden bestod i å redusere den proporsjonale forsterkningen i henhold til SIMC-tuningreglene. Dette resulterte i en betydelig reduksjon i amplituden til oscillasjonene i reaktortemperaturene, og dermed en mer stabil ytelse.

Avslutningsvis ble kaskaderegulering implementert. For den indre sløyfen ble katalysatortemperaturen benyttet, da denne hadde en raskere respons p gassammensetningsforstyrrelser. For den ytre sløyfen ble reaktorutløpstemperaturen benyttet, slik som i det eksisterende anlegget. Denne reguleringsstrukturen ga de mest optimale resultatene, da den har mulighet til kompensere for forstyrrelsen før den detekteres i utløpstemperaturen.

Contents

1 Introduction **1**
1.1 Scope of work . . . 2

2 Background **2**
2.1 Process description . . . 2
2.1.1 Heat exchanger . . . 4
2.1.2 Electric heater . . . 4
2.1.3 Catalytic incinerator . . . 4
2.2 Process control . . . 5
2.2.1 General . . . 5
2.2.2 PID control . . . 6
2.2.3 Performance of PID controllers . . . 9
2.2.4 The SIMC PID tuning method . . . 9
2.3 Controllability and control improvement . . . 11
2.3.1 Controllability . . . 11
2.3.2 Cascade control . . . 12

3 Modeling of the process **13**
3.1 Assumptions . . . 13
3.2 Model equations . . . 13
3.2.1 Heat exchanger . . . 14
3.2.2 Electric heater . . . 16
3.2.3 Catalytic incinerator . . . 16
3.2.4 Misc. (pipes, airmixer etc) . . . 18

4 Parameter fitting and open loop simulations **19**
4.1 Implementation in Matlab/Simulink . . . 19
4.2 Model adjustments . . . 20
4.2.1 Heat exchanger . . . 20
4.2.2 Catalytic incinerator . . . 21

5 Current control structure **24**
5.1 The control loops . . . 24
5.1.1 TIC-1401B . . . 26
5.1.2 Temperature controller TIC-1401A . . . 27

5.2 Temperature controller TIC-1402 27
5.3 Analysis of current control structure 28

6 Control improvement **31**
6.1 Simulation of current control structure 31
6.2 Control improvement 33
6.2.1 Re-tuning of TIC-1402 33
6.2.2 Cascade control 33

7 Discussion **37**
7.1 The model 37
7.1.1 General 37
7.1.2 The catalytic incinerator 37
7.2 The control aspect 38

8 Conclusion **40**
8.1 Further work 40

A SIMC re-tuning of TIC-1402 **42**

B Cascade controller tunings **43**
B.1 Inner loop 43
B.2 Outer loop 44

C P&ID of process **46**

D Gas composition variations **47**

E Some examples of the Matlab code **48**
E.1 Parameters 48
E.2 Heat exchanger model 50
E.3 Heat exchanger s-function 53
E.4 Incinerator model 54

List of Figures

1 P&ID of the catalytic waste incineration plant at Perstorp. 3
2 The different basic control systems. 6
3 Block diagram representation of a proportional controller. 7
4 Block diagram representation of a PID controller. 7
5 Estimation of model data using an open-loop step response. 10
6 Block diagram representation of cascade control. 12
7 Schematic representation of the structure of the heat exchanger model.hexmod . 14
8 Schematic representation of the structure of and the mechanisms included in the reactor model, except the heat of reaction. 16
9 The open-loop process model implemented in Simulink. 19
10 Real temperature measurements during operations of heat exchanger H-141, 27.10.2010. The figure shows the inlet and outlet temperatures of the hot and cold side, respectively. 21
11 Steady-state simulation of the heat exchanger, with a gas flow rate of 1800 Nm^3 on both sides, a water content of 2 wt% and both the shell and tube side heat transfer coefficients set to 40 W/m^2C 21
12 Real temperature measurements during operations of catalytic incinerator E-140. The plots show the temperature inside the catalyst bed (TI1403) and at the reactor outlet (TIC1402) as a function of time, for 13.04.2010 (top) and 01.01.2010 (bottom). 22
13 Simulation of the catalytic incinerator with a catalyst mass of 280 kg. The top figure shows the response in the bed and outlet temperature for a sinusoidal disturbance in the VOC concentrationwith an amplitude of 0.6 wt%. The bottom figure shows the corresponding response for a step in the air flow from 0 to 1 kg/s at t = 300 min. 24
14 Simulation of the catalytic incinerator with a catalyst mass of 280*5 kg. The top figure shows the response in the bed and outlet temperature for a sinusoidal disturbance in the VOC concentrationwith an amplitude of 0.4 wt%. The bottom figure shows the corresponding response for a step in the air flow from 0 to 1 kg/s at t = 300 min. 25
15 - Schematic representation of the current control structure at Perstorp catalytic waste incineration plant. 26
16 Temperature measurements and control signals logs from 13.04.2010. 29
17 The control structure implemented in Simulink. 31
18 Simulation results using controller parameters in table 4. The disturbance has a period of 50 min in the top figures and 100 min in the bottom figures, and an amplitude of 0.03 wt% VOC and a bias of 0.9 wt%. A step in the bias from 0.9 wt% to 1.1 wt% is introduced at t = 600 min. 32

19 Simulation results using controller parameters in table 5. The disturbance has a period of 50 min in the top figures and 100 min in the bottom figures, and an amplitude of 0.03 wt% VOC and a bias of 0.98 wt%. A step in the bias from 0.98 wt% to 1.18 wt% is introduced at t = 600 min. 34
20 Simulation results using cascade control. The disturbance has a period of 50 min in the top figures and 100 min in the bottom figures, and an amplitude of 0.03 wt% VOC and a bias of 0.9 wt%. A step in the bias from 1.0 wt% to 1.2 wt% is introduced at t = 600 min. 35
A.1 Step response of outlet temperature for re-tuning of TIC-1402. 42
B.1 Step response of temperature in catalyst bed used for tuning of the inner loop of the cascade controller. 43
B.2 Step response of temperature in reactor outlet used for tuning of the outer loop of the cascade controller. 44
B.3 The cascade structure in Simulink 45
C.1 P&ID of process. 46
D.1 Typical input concentration variations. 47

List of Tables

1 Controller settings for TIC-1401B. 27
2 Controller settings for TIC-1401A. 27
3 Controller settings for TIC-1402. 28
4 Controller parameters used to reproduce the existing control structure. The proportional gain is not scaled. 32
5 Controller parameters for TIC-1402 obtained by using the SIMC tuning rules. The proportional gain is not scaled. 33
6 Controller parameters used for cascade control structure. The proportional gain is not scaled. 35

1 Introduction

The Perstorp group is a world leader in several sectors of the speciality chemicals market, with sites located in different parts of the world. In this project, the site in Perstorp in Sweden is considered. With the industrial production of large quantities of speciality chemicals like alcohols, organic acids and formates come responsibilities regarding sustainability.

Perstorp believes that the environmental impact aspects that have the most significance from a global perspective are consumption of raw materials, energy and non-renewable resources, substances and consumption and contamination of water and emissions of greenhouse gases and volatile organic substances. This thesis focuses on the latter of these aspects.

Catalytic incineration of waste gases is a common way of treating chemical waste streams containing volatile organic substances that cannot simply be released to the atmosphere due to environmental restrictions. This method includes the complete combustion of said substances over a catalyst into carbon dioxide and water before the release to the atmosphere. The catalytic incinerators at Perstorp treat waste gases from various parts of the plant, depending on the activity. As a result, the composition of and concentration of the various organics in the gas may vary rapidly. This has demonstrated to make the process control at the incinerators at Perstorp challenging.

A functional process control structure is of huge importance for several reasons - for optimal operation, for minimization of energy usage and for safety. Excessive increases in temperature, for instance, may cause severe damage to process equipment with costly reparations and operations downtime. Too low temperature, on the other hand, may cause emission of harmful substances due to incomplete combustion.

Due to the rapid composition variations in the inlet gas, the incinerators at Perstorp have had issues with absorption of organic compounds to the catalyst bed. This may lead to explosions due to rapid increase in temperature when they subsequently desorb and combust. The central objective of the control system is thus to keep the temperature in the incinerator as stable as possible by manipulating the gas concentration using air.

1.1 Scope of work

The main objectives of this work are the development of a mathematical model which represents the dynamic behaviour shown at the incinerator at Perstorp's plant. An identification of the main current control issues and limitations will be performed. Finally, the possibilities of improvement of the control structure for more stable operation will be investigated.

2 Background

2.1 Process description

The process considered in this project is a catalytic incinerator at Perstorp, Sweden. The incinerator treats waste gases from various parts of the plant, like crystallizers, reactors, distillation columns and vacuum systems, and is designed to handle 1800 Nm3/h of gas. The organic substance present in the waste gases is mainly MIBK (methyl isobuthyl ketone), but also other volatile organic compounds (VOC) like metachrolein, methanol, methylal and methyl formate. The composition and origin of the waste gases varies depending on the activity at the plant. The concentration of VOCs in the waste gases is of the order of magnitude of 0.5 wt%, while the rest of the gas consists mainly of air and also some water.

A schematic representation of the process is shown in figure 1. A larger version is shown in appendix C.

The waste gases are transported from the production facilities and through the waste gas treatment facility by a fan. The gases are first passed trough the tube side of heat exchanger H-141, where they are preheated by the hot treated gases which pass through the shell side. The heat exchanger has a hot side bypass in order to control the transferred heat. After passing through the heat exchanger, the waste gases are led to the electric heater E-141 where the gas temperature can be increased to the required inlet temperature for reactor E-140. If the organics content of the waste gases exceeds 6.5 g/Nm3 at a flowrate of 1800 Nm3/h, the catalytic incineration plant is autothermal, which means that there is no need for electrical heating in E-141. Otherwise, the electric heater is needed to achieve a sufficiently high temperature such that all VOC reacts.

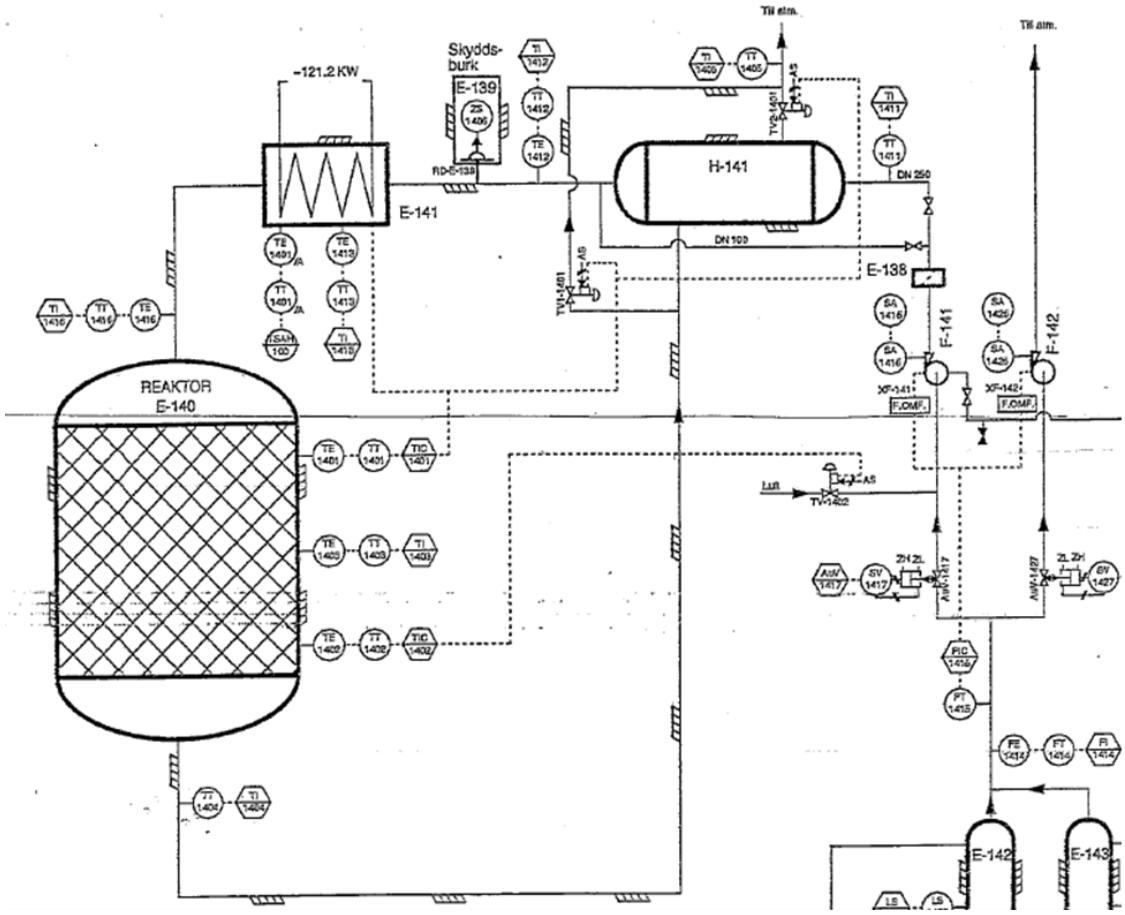

Figure 1: P&ID of the catalytic waste incineration plant at Perstorp.

After leaving the electric heater, the waste gases are passed through the catalytic incineration reactor E-140. In the reactor, the organic compounds are combusted to CO2 and water under the influence of a VOC oxidation catalyst. The combustion is exothermic, and thus leads to a temperature increase throughout the reactor. This temperature increase is proportional to the amount of organics in the gases.

It is important to ensure that the temperature of the waste gases is above 250C before entering the reactor. This is to avoid adsorption of organic compounds to the catalyst. The adsorbed compounds will subsequently desorb when the temperature in the reactor increases. This sudden increase in concentration of gaseous organic compounds in the reactor results in a large amount of heat being released from the combustion, which may in the worst case cause an explosion.

The VOC oxidation catalyst in reactor E-140 ensures that a cleaning efficiency of above 99 % can be achieved at a temperature of 270 C. Thus, it is also important to keep the temperature of the inlet gases sufficiently high in order to ensure complete combustion of the organics. On the other hand, the temperature of the hot outlet gases should be kept below 420 C in order to avoid damaging the catalyst and other process equipment. This is ensured by diluting the waste gas stream with atmospheric air through the air bleed valve when necessary.

Finally, the hot purified exhaust gases from reactor E-140 are passed through the shell side of heat exchanger H-141 to preheat the incoming gas, and released to the atmosphere.

2.1.1 Heat exchanger

The heat exchanger is a countercurrent shell and tube gas-gas heat exchanger. In order to be able to control the cold side temperature, it has a hot side bypass.

The heat exchanger has 349 tubes with an inner diameter of 1.5 cm. The heat transfer area is 115 m^2. The shell side is insulated.

The parameters used in the simulations are shown in appendix E.

2.1.2 Electric heater

The electric heater is a standard duct heater with tubular heating elements. The container itself is constructed in stainless steel, and is insulated.

The heater has an electrical effect of 120.1 kW.

The parameters used in the simulations are shown in appendix E.

2.1.3 Catalytic incinerator

The catalytic incinerator is cylindrical and constructed in stainless steel, is insulated and has a diameter of approx. 1.4 m. Inside the reactor there is a catalyst bed with 280 kg of 4.0-6.7 mm pellets of the oxidation catalyst PPt-47, which has platinum as the active component on an alumina carries. The height of the catalyst bed is 0.33 m.

The disturbances which directly affect the temperatures inside the reactor are the gas flow rate, the mass fraction of combustible organics and the inlet temperature of the gas to the reactor.

The parameters used in the simulations are shown in appendix E.

2.2 Process control

2.2.1 General

Control refers to the regulation of given aspects of a process. In many applications, it is of high importance to be able to precisely control e.g. levels, temperatures, pressures or flow rates. Thus, process control refers to methods which are applied in order to control such process variables when running a process or manufacturing a product.

The three main goals of process control are:

- Setpoint tracking. The variable should follow some prespecified path in time. This might be because a certain trajectory of the operating point maximizes the efficiency of the process.
- Disturbance rejection and reduction of variability. Compensating for various disturbances affecting the process output is important for predictability and consistency of the quality of the process output.
- Ensure safety. Processes that may risk thermal runaway or increasing pressures in boilers are examples of aspects that may threaten the environment and workers' safety if not controlled properly.

Two basic types of control systems are open-loop and closed-loop systems, where closed-loop systems can generally be divided into feed-forward and feedback systems. These 3 control systems are shown using block diagram representations in figure 2.

Open-loop control is the simplest form of control: it only uses the current state and a model of the system to calculate its input. Thus, it cannot compensate for disturbances in any way.

Using feed-forward control, the disturbances are measured and accounted for before they have the time to affect the system. However, the affect of the disturbances on

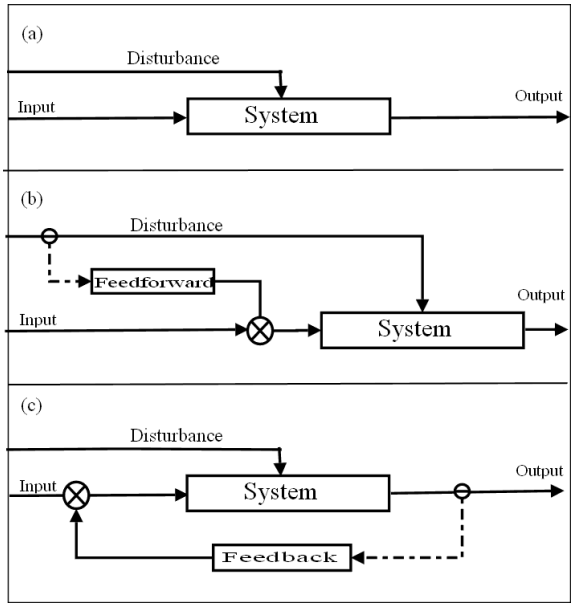

Figure 2: The different basic control systems.

the system must be accurately predicted, and thus an accurate mathematical model of the relationship between the disturbance and the output is required. In addition, there cannot be any unmeasured disturbances.

The feedback structure has the advantage that the controller is error-driven, and therefore automatically compensates for disturbances. Thus, no detailed mathematical model of the relationship between the disturbance and the output is required for good performance. However, feedback control is limited in that it can only take corrective action once the error from the disturbance is detected in the process output. This is highly important for the controller performance when there is a significant deadtime between the measured output variable and the input or manipulated variable.[1]

2.2.2 PID control

The simplest feedback controller available, except for the on-off-controller, is the proportional controller. This is a linear controller where the control signal u is proportional to the control error e, as shown in figure 3.

The equation that describes the output signal from a proportional controller is in the time domain given by:

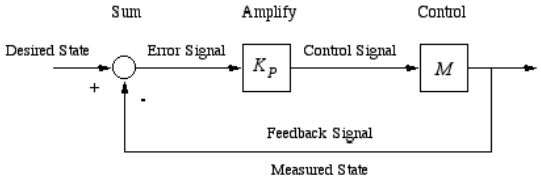

Figure 3: Block diagram representation of a proportional controller.

$$u(t) = Ke(t) \tag{1}$$

where K is the proportional gain and e is the control error, given by:

$$e(t) = y_s(t) - y(t) \tag{2}$$

where $y_s(t)$ is the setpoint and $y(t)$ is the controlled variable or measurement.

This shows that there has to be an error in order to produce a controller output. Consequently, using a proportional controller will always produce an offset between the measured variable and the setpoint at steady-state. As a result, a more complex control algorithm than pure proportional control is normally used in order to eliminate this offset.

The PID controller, or proportional-integral-derivative controller, is one of the most commonly used control algorithms in industry, and has been used since the 1930's. The controller block diagram in the time domain is shown in figure 4.

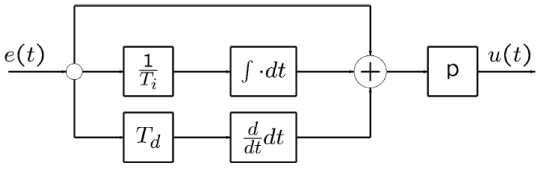

Figure 4: Block diagram representation of a PID controller.

The PID algorithm can be described as follows in the time domain:

$$u(t) = K\left(e(t) + \frac{1}{\tau_i}\int_0^t e(\tau)\,\mathrm{d}\tau + \tau_d\frac{\mathrm{d}e(t)}{\mathrm{d}t}\right) \tag{3}$$

where e is the control error, τ is a variable of integration which takes on values from $t = 0$ to the present time, K is the proportional gain, T_i is the integral time and T_d is the derivative time.

The controller output u is a sum of three terms: the P-term which is proportional to the error, the I-term which is proportional to the integral or duration of the error, and the D-term which is proportional to the derivative or the rate of change of the error. The controller or tuning parameters are thus the proportional gain K , the integral time τ_i and the derivative time τ_d .

A high proportional gain results in a large change in the controller output for a given current value of the error.

The proportional gain of the controller gain can be of either positive or negative value, depending on the gain of the process. If the process gain is positive, an increase in the value of the controller or measured variable y requires a decrease in the control signal u in order counteract the change in the controlled variable y away from the setpoint y_s. In this case, the controller gain K needs to be positive, due to the definition of the control error as given in equation 2. This is called reverse-acting control. In the second case, with a negative process gain, an increase in the value of y requires an increase in u. In this case the controller gain needs to be negative. This is called direct-acting control.

The main purpose of integral action is to eliminate offset. It continues to change the controller output as long as an error exists. The longer the integral time, the lower is the I-action and thus the slower the measured variable moves towards the setpoint.

Derivative action is intended to be anticipatory. The error may be very small, but if it changes rapidly, it will be large in the future. Thus, the derivative action tries to prevent this by changing the output in proportion to the rate of the change of the error. The higher the derivative time, the more influence the change of the error has on the controller output.[1]

In addition, the derivative term is often not applied in industry. This is because this

term is very sensitive to measurement noise. In this case, the controller is called a PI-controller.

2.2.3 Performance of PID controllers

As mentioned in section 2.2.1, one of the main limitations of feedback controllers is dealing with processes with a significant dead-time. No corrective action is taken before the error from the disturbance is actually detected in the process output. Thus, perfect control is not achievable using feedback control only. The disturbance will always, to some degree, have some time to increase the error before the controller has the chance to react.

Saturation is also a limitation for control. Saturation occurs when the actuator for a manipulated variable, for example a valve, is either fully open or fully closed and the sepoint still cannot be reached. Thus, further control is not possible as the manipulated variable can no longer affect the measured variable.

2.2.4 The SIMC PID tuning method

Although PID controllers have only 3 tuning parameters, it can be surprisingly difficult to find good values or tunings for them without a systematic approach. Several methods for tuning PID controllers are available in the literature, like the Ziegler-Nichols and the Cohen-Coon methods.

Another tuning method is called the Skogestad Internal Model Control (SIMC) method. This method was developed by Prof. Sigurd Skogestad with the objective to be simple and easily memorizable, while still providing good controller performance and versatility. It should also be well motivated, model-based and analytically derived.

In short, this method has only one tuning parameter - the desired first order *closed-loop* time constant, τ_c.

The controller tunings obtained by this method are based on approximating the process by a first- or second order model with the following model information:

- Plant gain, k
- Dominant time constant, τ_1

- (Effective) dead time, θ

These data can be obtained in several ways: estimated from an open-loop step response, from a closed-loop response with a P-controller or identified from a detailed model where the effective dead time is approximated using the half rule. The first of these methods is shown in figure 5.

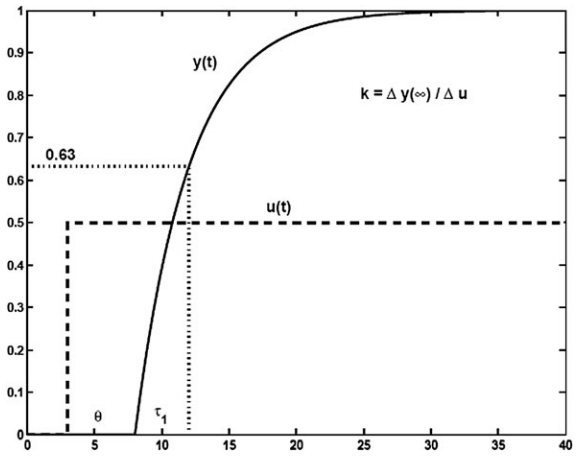

Figure 5: Estimation of model data using an open-loop step response.

Using the open-loop step response method, the model can in the frequency domain be approximated as a first-order model plus time delay on the form

$$g(s) = \frac{k}{\tau_1 s + 1} e^{-\theta s} \tag{4}$$

Further, the SIMC tuning rules may be derived using the Internal Model Control approach, where the desired closed-loop response is specified. In short, the SIMC tuning rules are summarized as follows. For a first order model, the SIMC method results in a PI controller with the settings

$$K = \frac{1}{k} \frac{\tau_I}{\tau_c + \theta} \tag{5}$$

$$\tau_I = min\{\tau_1, 4(\tau_c + \theta)\} \tag{6}$$

where k is the steady state plant gain and τ_1 is the first order time constant as shown in figure 5.τ_c is the desired closed loop time constant, which is the only tuning parameter. [2]

2.3 Controllability and control improvement

2.3.1 Controllability

There can be many reasons why a process control structure doesn't provide sufficient performance. First of all, it is important to identify the control characteristics of the process itself.

According to Skogestad [3] "*Input-Output controllability is the ability to achieve acceptable control performance, that is, to keep the outputs (y) within specified bounds or displacements from their references (r), in spite of unkown but bounded variations, such as disturbances (d) and plant changes, using available inputs (u) and available measurements (y_m or d_m).*"

Thus, a plant is controllable if there exists a controller that provides acceptable performance for all expected plant variations. This means that the term "controllability" is independent of the controller, and is a property of the process alone. The only way to affect the controllability, is to change the plant itself. These changes may include changing the apparatus itself (type, size etc.), relocating sensors and actuators, adding extra sensors and actuators, adding new equipment to dampen disturbances, changing the control objectives and/or changing the configuration of the lower control layers that already in place. For example, the size of a buffer tank can be increased in order to reduce the effects of a disturbance. [3]

If the plant is input-output controllable using the existing control configuration and the performance is still insufficiently good , one should evaluate the current controller tunings. For example, if the proportional gain is too low, the system response becomes too sluggish. If is set too high, however, the system will overshoot, oscillate and in a worst-case scenario become unstable.

2.3.2 Cascade control

Another way to improve the performance of PI-controllers is by application of so-called cascade control. In cascade control, two PI-controllers are used together in order to improve the overall dynamic behaviour of the system. One controller, called the primary controller, adjust the setpoint of a secondary controller. This control structure is applied when the process dynamics are such that the secondary or inner-loop controller can detect and thus compensate for a disturbance significantly faster than the primary or outer-loop controller.[1]

A block diagram representation of a cascade control structure is shown in figure 6.

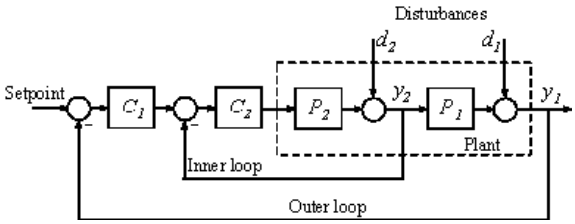

Figure 6: Block diagram representation of cascade control.

3 Modeling of the process

3.1 Assumptions

The following assumptions apply to the entire model.

The density of the gas in each lumped element in the model is computed using the ideal gas law:

$$\rho_g = \frac{PM}{RT} \tag{7}$$

where P is the given pressure in atm, M is the molecular mass in the gas in kg/mol, R is the universal gas constant in m^3atm/Kmol and T is the temperature in K.

Further, as the VOC content of the gas is very low, the molar mass and heat capacity of the gas is assumed to be those of pure air. In addition, these values are treated as constants.

As all process equipment is well isolated, no heat loss to the environment is included in the model.

3.2 Model equations

In order to avoid the complicated partial differential equations, the heat exchanger and the reactor were modelled as a series of lumped systems. This means that instead of introducing a spatial or axial derivative, the process is divided into a series of N connected lumps or CSTRs which are assumed to be perfectly mixed and thus have no gradients. Thus, the temperature and other states of the stream exiting a given lump are identical to the states inside the lump. Using this approach, each lump represents a spatial position in the system. If the number of CSTRs is high enough, this system's response is close to the one of a distributed system.

Using the lumped system method, a general energy balance over a control volume V is given as

$$\rho V c_p \frac{dT}{dt} = \sum_{\forall m} \alpha_m \sum_{\forall i} (h_{i,m} - h_i)\hat{n}_{i,m} + \sum_{\forall m} \alpha_m p_m \hat{V}_m + \sum_{\forall q} \alpha_q \hat{q}_q + \sum_{\forall w} \alpha_w \hat{w}_w \quad (8)$$

The left hand side represents change of internal energy in the given CSTR with respect to time, while the right hand side represents the different mechanisms in which heat is supplied to or removed from the system : due to mass flows, heat flows and work flows.

The electric heater and process gas/air mixing volume were also modelled in this way, only with one single lump for the gas phase only.

3.2.1 Heat exchanger

The countercurrent heat exchanger with a hot side bypass is modelled using the lumped systems approach. This means that the cold gas side, the hot gas side and the heat transfer wall are divided into a number of N lumped elements. This modelling approach has been found to provide realistic dynamic behaviour, according to Mathisen [4]. A schematic representation of the model is shown in figure 3.2.1.

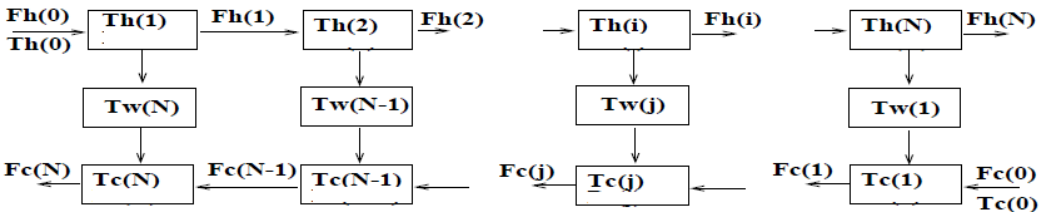

Figure 7: Schematic representation of the structure of the heat exchanger model.hexmod

It is assumed that there is no conductive heat transfer between the different heat exchanger wall elements, and that the wall has constant specific heat capacity. The pressure drop is also assumed to be negligible.

The heat transfer coefficient between the gas and the wall is assumed constant and equal on both the hot and the cold side of the exchanger.

In addition, the real operation data show a larger temperature difference on the hot side than on the cold side, as shown in figure 10, which may be due to evaporation of water

droplets in the cold side inlet stream. This is included in the model. The evaporation is assumed to take place in only one element.

The model equations for the heat exchanger are thus

for each element i of the cold side fluid:

$$\frac{\rho_g V_c c_{p,g}}{N}\frac{dT_c(i)}{dt} = (\dot{m}_g + \dot{m}_{air})c_{p,g}(T_c(i-1) - T_c(i)) - \frac{h_w A_w}{N}(T_c(i) - T_w(N+i-1)) - \delta\omega_{H_2O}\dot{m}_g\Delta_{vap}H_{,H_2O} \tag{9}$$

where

$\delta = 1$ in the element in which the evaporation is assumed
$\delta = 0$ in all other elements

and

ρ_g is the gas density [kg/m3], V_c is the cold side volume [m3], $c_{p,g}$ is the specific heat capacity of the gas [J/kgC], T_c is the cold side temperature [C], $\dot{m}_g$ and $\dot{m}_{air}$ are the mass flows of waste gas and air [kg/s], h_w is the wall heat transfer coefficient [W/m2C], A_w is the heat transfer area [m3], T_w is the wall temperature [C], ω_{H_2O} is the mass fraction of water in the gas [-] and $\Delta_{vap}H_{,H_2O}$ is the heat of vaporization for water [J/kg],

and for the hot side fluid:

$$\frac{\rho_g V_h c_{p,g}}{N}\frac{dT_h(i)}{dt} = (1-\alpha)(\dot{m}_g + \dot{m}_{air})c_{p,g}(T_h(i-1) - T_h(i)) - \frac{h_w A_w}{N}(T_h(i) - T_w(i)) \tag{10}$$

where α is the bypass fraction and the subscript h denoted hot side,

and finally for the wall elements:

$$\frac{m_w c_{p,w}}{N}\frac{dT_w(i)}{dt} = \frac{h_w A_w}{N}[(T_c(N+i-1) - T_w(i)) + (T_h(i) - T_w(i))] \tag{11}$$

where m_w and $c_{p,w}$ represents the mass [kg] and the specific heat capacity [J/kgC] for the heat exchanger wall.

3.2.2 Electric heater

The electric heater is modelled simply as a single lumped system without any gradients. The energy is supplied directly to the gas phase. This is reasonable to assume as electric heating elements have a rapid response, and the heat transfer conditions between the elements and the air is usually optimally constructed.

The equation for the temperature in the gas exiting the heater is thus

$$\rho_g V_{el} c_{p,g} \frac{dT_{out}}{dt} = \dot{m} c_{p,g} (T_{in} - T_{out}) + \dot{W} \tag{12}$$

where V_{el} represents the gas volume inside the heater [m3] and $\dot{W}$ the added effect [J/s].

3.2.3 Catalytic incinerator

The catalyst bed consists of the moving gas phase and the stagnant solid catalyst phase, as shown in figure 8

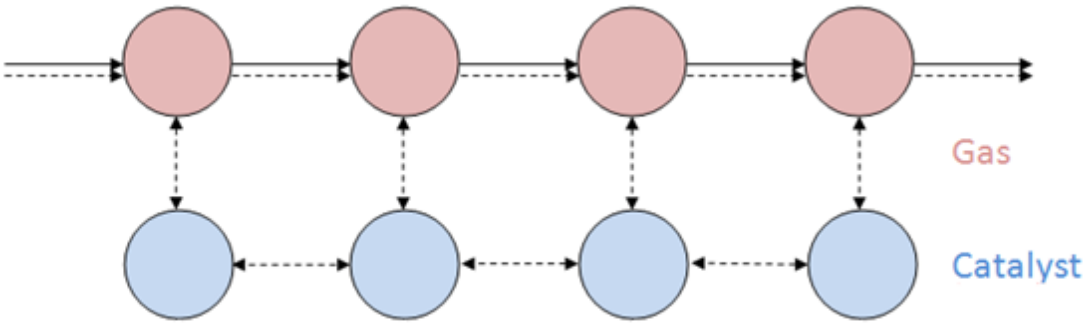

Figure 8: Schematic representation of the structure of and the mechanisms included in the reactor model, except the heat of reaction.

The mechanisms which are included in the model can be seen from figure 8. These are convective mass transfer in the gas phase, convective heat transfer in the gas phase, heat of reaction in the gas phase, heat transfer between the gas- and catalyst phase and conductive heat transfer in the catalyst phase.

As no heat loss is assumed in the model, the temperature of the gas volume after the catalyst bed will be the same as the temperature of the gas in the final element in the catalyst bed.

The heat transfer coefficient between the gas and catalyst phase is assumed constant.

The following assumptions were made regarding the exothermic reaction:

- The reaction happens instantaneously the element in which the catalyst temperature exceeds the ignition temperature, which is 270C.
- The reaction reaches 100% conversion, i.e. it is not limited by equilibrium.
- The reaction occurs in the catalyst phase.

Applying these assumptions, a general energy balance for the system yields for each i element of the gas phase

$$\frac{\rho_g(i)V_g c_{p,g}}{N}\frac{dT_g(i)}{dt} = ((\dot{m}_g + \dot{m}_{air})c_{p,g}(T_g(i-1) - T_g(i)) - \frac{(UA)_{cat}}{N}(T_g(i) - T_{cat}(i)) \tag{13}$$

and for each element i in the catalyst phase

$$\frac{m_{cat}c_{p,cat}}{N}\frac{dT_{cat}(i)}{dt} = \frac{(UA)_{cat}}{N}(T_g(i) - T_{cat}(i)) + (kA/L)_{cat}N(T_{cat}(i-1) + T_{cat}(i+1) - 2T_{cat}(i)) + (\dot{m}_g\omega_{VOC}\Delta \tag{14}$$

where

$\delta = 1$ in the element in which the reactor occurs and
$\delta = 0$ in all other elements

where N is the number of lumped elements, $T_g(i)$ and $T_{cat}(i)$ are the temperatures of

the gas and catalyst phase in lump i, respectively [°C], $c_{p,g}$, $\rho_g(i)$ is the density of the gas phase in element i calculated using equation X [kg/m^3] $c_{p,cat}$ are the heat capacities of the gas phase and catalyst phase, respectively [J/kg°C], V_g is the volume of the gas phase in the reactor [m^3], $\dot{m}_g$ is the mass flow rate of process waste gas [kg/s], $\dot{m}_{air}$ is the mass flow rate of air added to the waste gas stream [kg/s], m_{cat} is the mass of catalyst [kg], $(UA)_{cat}$ is the heat transfer coefficient times heat transfer area between the gas and the catalyst [W/°C], $(kA/L)_{cat}$ is the thermal conductivity of the catalyst times the height of the catalyst bed [W/°C],

3.2.4 Misc. (pipes, airmixer etc)

The air is supplied directly to the waste gas stream. The air stream and the waste gas stream are assumed to be perfectly mixed in a given volume where they meet. An energy balance over this volume yields

$$\rho_g V_{mix} \frac{dT_g}{dt} = \dot{m}_g T_{g,in} + \dot{m}_{air} T_{air} - (\dot{m}_g + \dot{m}_{air}) T_g \tag{15}$$

where V_{mix} is the mixing volume [m3] and the subscript *air* refers to atmospheric air being supplied to the process.

The pipes are modelled simply as variable transport delays of the states of the gas flows entering the pipes. The lengths of the pipes are fixed, and thus the transport delays are given by the flow rate of gas through the pipes:

$$t_d = \frac{L_{pipe}}{v_g} = \frac{L_{pipe} \rho_g S_{pipe}}{(\dot{m}_g + \dot{m}_{air})} \tag{16}$$

where L_{pipe} is the length of the pipe [m] and S_{pipe} is the pipe cross section [m3].

4 Parameter fitting and open loop simulations

4.1 Implementation in Matlab/Simulink

The softwares used to simulate the model in this project are Matlab and Simulink, both developed by MathWorks. Matlab is a numerical computing environment and programming language. Simulink is block diagram environment for modeling, simulating and analyzing dynamic systems widely used in control theory and signal processing.

The differential equations describing the system in this project could have been built directly in Simulink using predefined blocks. However, this does not provide a very flexible model. For example for models consisting of a series of lumped systems, increasing or decreasing the number of lumped elements is an inconvenient and time-consuming task as the number of differential equations increases or decreases. Thus, it was decided to combine the flexibility of Matlab and the control simulation conveniency of Simulink for this project. The system equations for each unit were written in Matlab separately, and were further implemented in Simulink using s-functions for custom blocks. The system units were connected in Simulink order to simulate the complete system.

Figure 9 shows the open-loop process model block diagram implemented in Simulink.

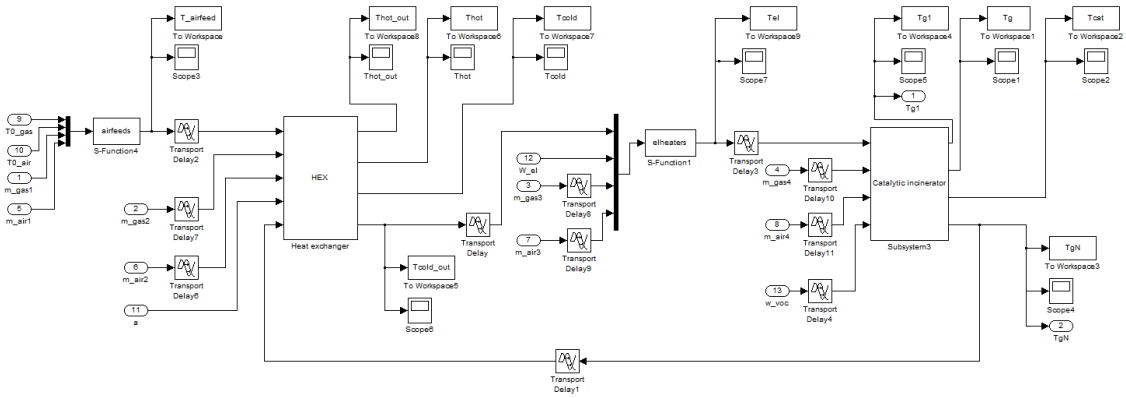

Figure 9: The open-loop process model implemented in Simulink.

An s-function, or system function, is a computer language description of a Simulink block written in Matlab, C, C++ or Fortran. S-functions provide a powerful mechanism for extending the capabilities of the Simulink environment. They are written in Matlab

and use a special calling syntax that enables you to interact with the Simulink engine. This interaction is very similar to the one which takes place between the Simulink engine and the already built-in Simulink blocks. [5]

4.2 Model adjustments

This chapter will cover the simulations done in order to adjust the model to fit the real operation data as closely as possible, both dynamically and stationary.

4.2.1 Heat exchanger

Most of the design data for the heat exchanger, like heat transfer area, construction materials, mass and volumes are provided by Perstorp and thus known. The main parameter that needs to be adjusted in order to match operation measurements is the heat transfer coefficient, which mainly affects the steady-state behaviour of the unit.

In addition, as mentioned in section 3.2.1, evaporation of water on the cold side may cause the deviation between the cold side and hot side temperature differences. The water content in the gas was adjusted to match this deviation.

Figure 10 shows the temperatures measured around the heat exchanger during plant operation, when the hot side bypass is rarely open and the waste gas flowrate is close to the one in the base case. The plots of the corresponding flowrate and bypass valve opening are shown in appendix B.

Figure 10 shows that the inlet temperature on the cold and hot side at the end of the period is approximately 13.5 and 330 C, respectively. The corresponding flowrate is, as shown in appendix B, approximately 1800 Nm^3 or 0.645 kg/s. These inputs were used for the simulation.

Figure 11 shows the resulting steady-state temperatures from the adjusted model. These results were obtained by setting the water content to 2 wt% and the heat transfer coefficient on both the shell and tube side to 40 W/m^2C.

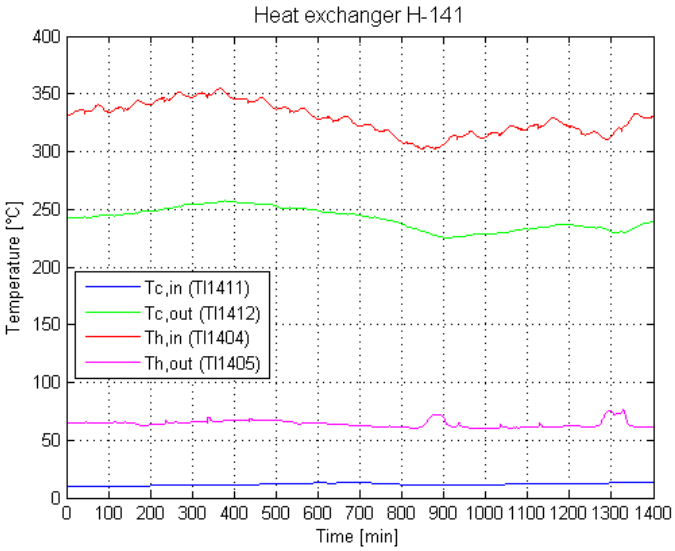

Figure 10: Real temperature measurements during operations of heat exchanger H-141, 27.10.2010. The figure shows the inlet and outlet temperatures of the hot and cold side, respectively.

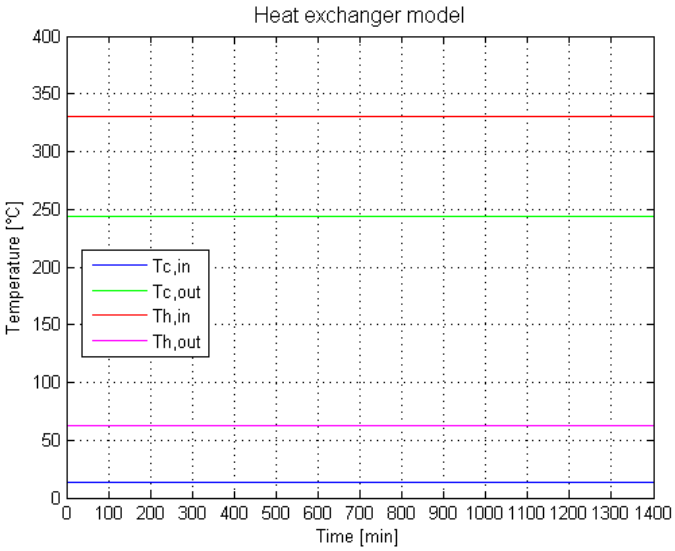

Figure 11: Steady-state simulation of the heat exchanger, with a gas flow rate of 1800 Nm^3 on both sides, a water content of 2 wt% and both the shell and tube side heat transfer coefficients set to 40 W/m^2C .

4.2.2 Catalytic incinerator

As for the heat exchanger, some data are also provided by Perstorp for the catalytic incinerator.

The following plots show the steady state and dynamic data of the temperatures within the catalytic incinerator. The model should as closely as possible show the same static and dynamic behaviour as the real system.

The steady state characteristic which is important is the difference between the gas outlet temperature and the temperature inside the catalyst bed, in other words the temperature peak inside the bed.

The dynamic charachteristics which characterize the dynamic behaviour of the system are the damping, the time constant and the delay of the disturbance oscillations throughout the reactor.

Figure 12 shows two days of operation logs of the temperatures throughout the catalytic incinerator. Additional measurements during the same days are given in appendix **??**

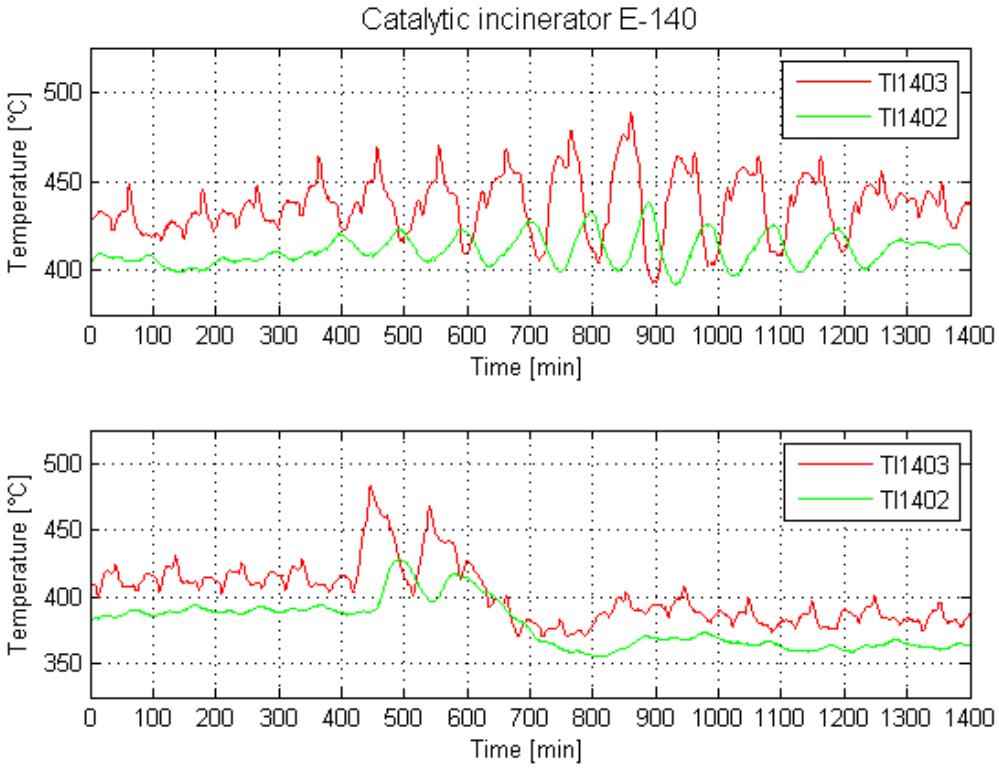

Figure 12: Real temperature measurements during operations of catalytic incinerator E-140. The plots show the temperature inside the catalyst bed (TI1403) and at the reactor outlet (TIC1402) as a function of time, for 13.04.2010 (top) and 01.01.2010 (bottom).

The main parameters that needed to be adjusted in order to provide the desired dynamics were the heat transfer coefficient between the catalyst bed and the gas phase and the inner thermal conductivity in the catalyst bed. The thermal conductivity of alumina catalyst particles beds are found in literature to be relatively low, but for a solid body of alumina it is in literature given as about 30 W/mK. Both the heat transfer between the catalyst phase and the gas phase determine the magnitude of the temperature peak inside the catalyst bed. An increase in the thermal conductivity will produce a smaller peak, and so will also an increase in the heat transfer. However, it was found that the heat transfer between the bed and the gas impacts the damping of the disturbance throughout the bed. A value of 20 000 W/K for the heat transfer coefficient times the heat transfer area and a value of 20 W/K for the conductivity was found to provide the desired result.

In order to investigate the resulting time delay and damping of disturbances throughout the reactor, a sinusoidal disturbance in the VOC concentration was introduced at t = 300 min. The disturbance had an amplitude of 0.6 wt%. In addition, a step in the air flow from 0 to 0.1 kg/s at t = 300 min was performed. The results are shown in figure 13.

However, with the catalyst mass of 280 kg provided, the apparent time delay of approximately 25 minutes throughout the reactor could not be achieved. This dead time might be of high significance when it comes to the control of the process. In addition, the damping of the sinusoidal disturbances was not captured. Thus, as it couldn't be captured using the mechanisms included in the model, it had to be introduced somehow. This could be done by either increasing the mass of the catalyst bed and thus the inertia of temperature change, or by introducing a pure time delay between the temperature in the bed and the outlet temperature. As the latter would not introduce the damping effect, the former approach was applied. Increasing the mass of the catalyst bed by a factor of 5, and also finally adjusting the heat transfer coefficient times are and the conductivity to 10 000 W/K and 30 W/K, respectively, provided a time delay and damping close to the ones observed at the real plant. The corresponding model results for this mass are shown in figure 14.

Thus, this model was used further in this project.

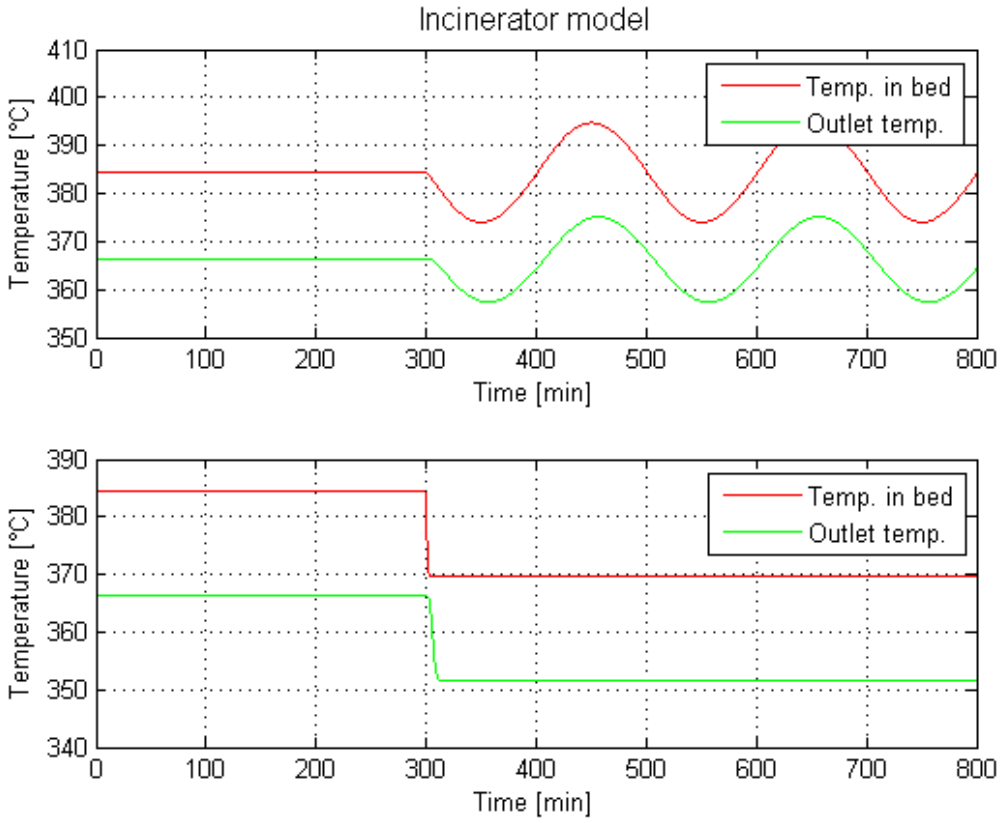

Figure 13: Simulation of the catalytic incinerator with a catalyst mass of 280 kg. The top figure shows the response in the bed and outlet temperature for a sinusoidal disturbance in the VOC concentrationwith an amplitude of 0.6 wt%. The bottom figure shows the corresponding response for a step in the air flow from 0 to 1 kg/s at t = 300 min.

5 Current control structure

5.1 The control loops

Figure 15 shows a schematic representation of the current control structure at the waste gas incineration plant.

As shown in the figure, there are 4 main control loops in this process: one pressure controller and three temperature controllers. The pressure controller was not modelled in this project, as it was considered implausible to be the source of the control difficulties.

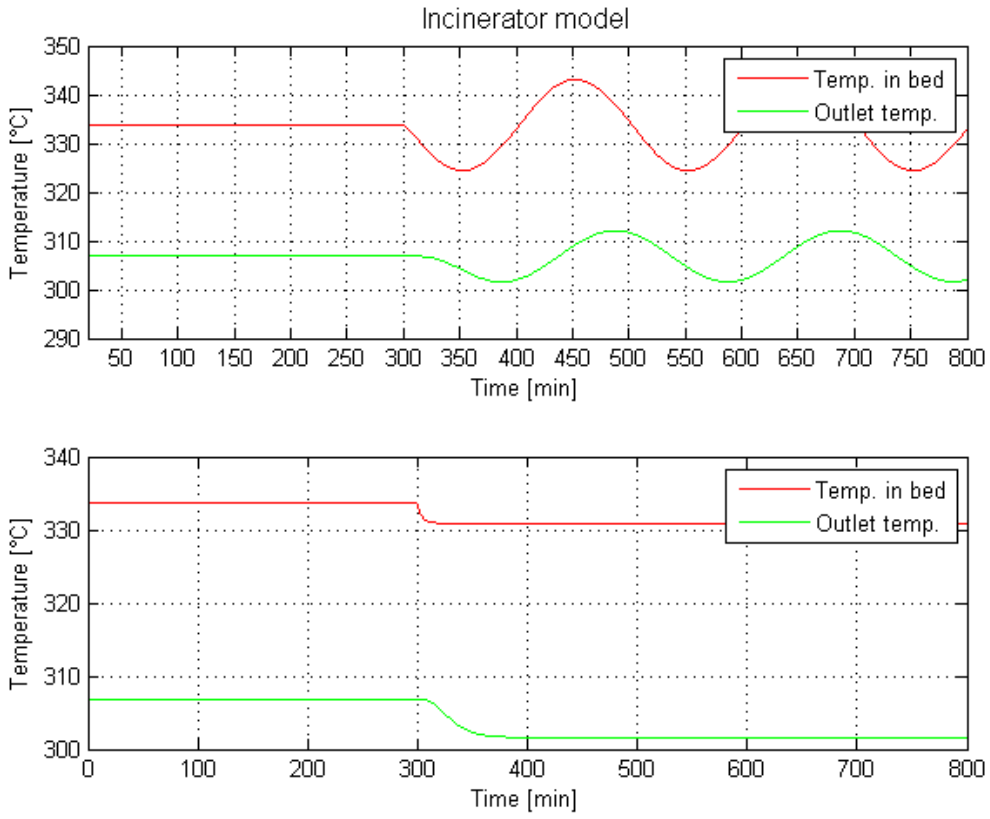

Figure 14: Simulation of the catalytic incinerator with a catalyst mass of 280*5 kg. The top figure shows the response in the bed and outlet temperature for a sinusoidal disturbance in the VOC concentrationwith an amplitude of 0.4 wt%. The bottom figure shows the corresponding response for a step in the air flow from 0 to 1 kg/s at t = 300 min.

The three temperature control loops were modelled and will be described in this section.

Temperature controllers TIC-1401A/B

Temperature controllers TIC-1401A and TIC-1401B control the inlet temperature of the gas to the reactor. Their purpose is to keep this temperature sufficiently high before it enters the catalyst bed, such that organic compontents do not adsorb to the catalyst surface.

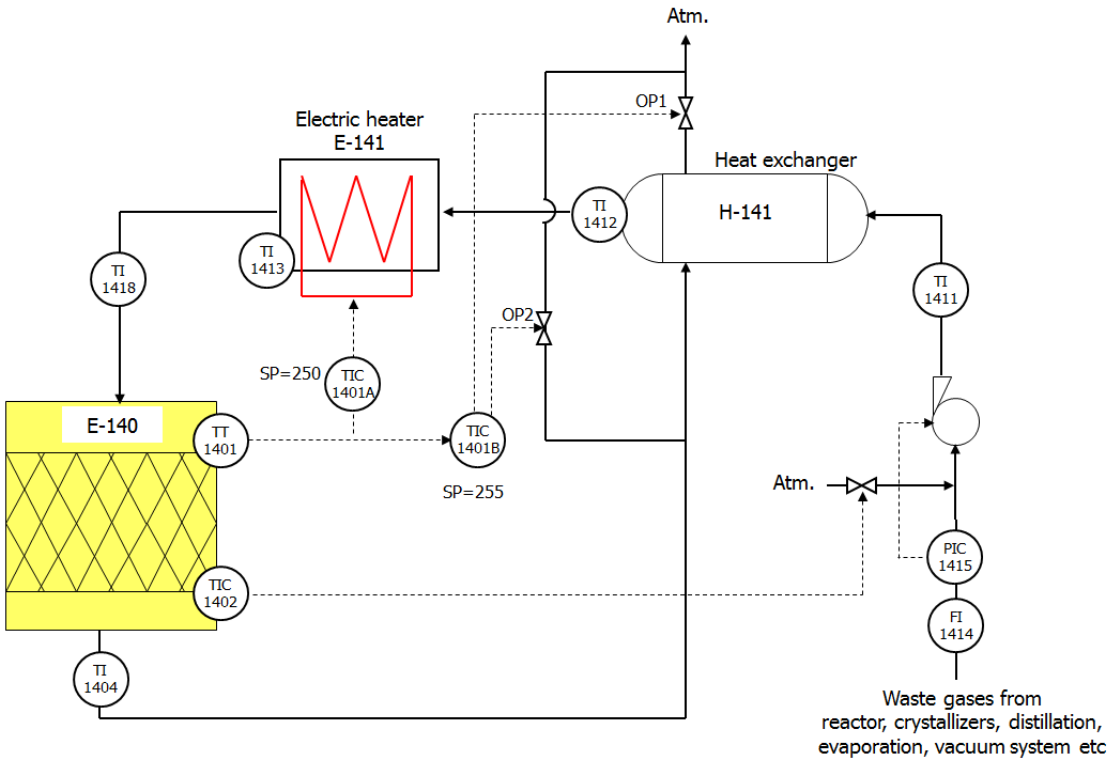

Figure 15: - Schematic representation of the current control structure at Perstorp catalytic waste incineration plant.

Hence, these two controllers have the same measured and controlled variable. However, their setpoints and manipulated variables are different. This will be explained in the following sections.

5.1.1 TIC-1401B

Temperature controller TIC-1401B controls the inlet temperature of the gas to the reactor by manipulation of the hot side bypass valves of the heat exchanger. Thus, it controls the temperature on the cold side by manipulation of the flow of hot outlet gases through the shell side of the heat exchanger.

The controller is a reverse-acting PI-controller. Its settings are shown in table 1.

Measured variable	Reactor inlet temperature
Controlled variable	Reactor inlet temperature
Manipulated variable	% of HEX bypass valve opening
Setpoint	255 C
Range	0-1000 C
K_p	11.11
T_i	1920 s
T_d	-

Table 1: Controller settings for TIC-1401B.

Measured variable	Reactor inlet temperature
Controlled variable	Reactor inlet temperature
Manipulated variable	% of max elheater effect (122.1 kW)
Setpoint	250 C
Range	0-1000 C
K_p	1
T_i	600 s
T_d	10 s

Table 2: Controller settings for TIC-1401A.

5.1.2 Temperature controller TIC-1401A

Temperature controller TIC-1401A also controls the inlet temperature of the gas to the reactor. It ensures that this temperature is sufficiently high by manipulation of the effect to the electric heater. Thus, this controller has the same measured and controlled variable as the heat exchanger bypass controller - however, its setpoint is somewhat lower. This way, electricity is only used when absolutely necessary, i.e. when the reactor inlet temperatur drops below this setpoint. As a result, the electric heater is rarely used and is only used if there is an insufficient amount of combustibles in the waste gas stream.

The controller is a direct-acting PID-controller. Its settings are shown in table 2.

5.2 Temperature controller TIC-1402

Temperature controller TIC-1402 controls the temperature of the gas at the outlet of the reactor, after it has passed through the catalyst bed. This is done by dilution of the waste gas stream by addition of air from the atmosphere.

Measured variable	Reactor outlet temperature
Controlled variable	Reactor outlet temperature
Manipulated variable	% of air inlet valve opening
Setpoint	420 C
Range	0-1000 C
K_p	8
T_i	2400 s
T_d	-

Table 3: Controller settings for TIC-1402.

As the inlet temperature to the reactor is kept constant by TIC-1401, the outlet temperature from the reactor is mainly a function of the concentration of combustibles in the waste gas stream. The higher the concentration, the higher the temperature increment due to the exothermic nature of the reaction.

The controller is a reverse-acting PI-controller. Its settings are shown in table 3.

5.3 Analysis of current control structure

Currently, there can be quite significant variations in temperatures in the system. Data logs of measured temperatures and flowrates throughout the process in addition to control signals show that severe oscillatory behaviour can sometimes be seen in the system.

Thus far it has not been clear what the exact origin of these variations are. Generally, the following scenarios were regarded as the main possibilities and investigated:

- The oscillations are mainly caused by one of the control loops alone
- The oscillations are mainly caused by disturbances of upstream origin
- A combination of the two former scenarios

In order to investigate which one of these scenarios that most likely applies to the process in question, the dynamic behaviour of the process and the controllers' responses to disturbances were obtained from operation data logs from the actual plant and studied.

The control loop for the electric heater, TIC-1401A, can immediately be disregarded as it is rarely active at all when the oscillations occur.

For this investigation, a day which had large temperature variations was chosen. The

temperature measurements and controller signals which the analysis is based on are shown in figure 16

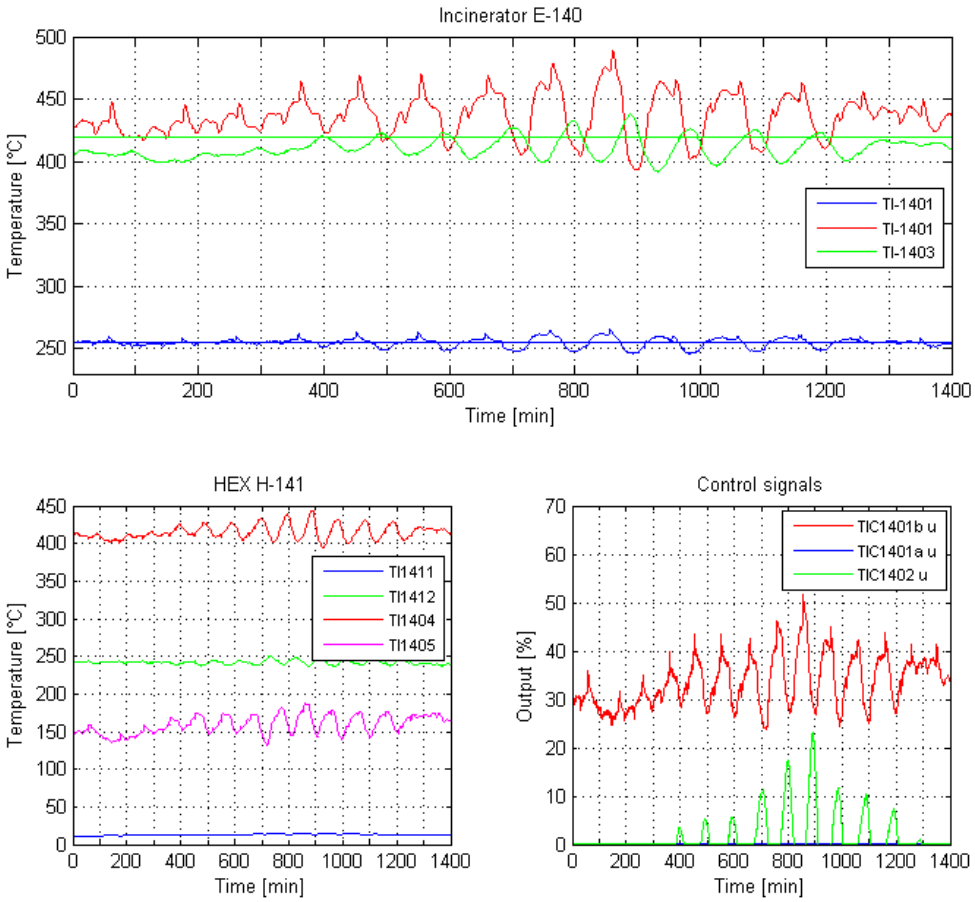

Figure 16: Temperature measurements and control signals logs from 13.04.2010.

Firstly, it was investigated whether or not the heat exchanger bypass controller could be the cause of the oscillations. Figure 16 shows that the cold side outlet temperature from the heat exchanger (TI1412) does not oscillate much compared to the temperature on the hot side (TI1404 and TI1405). Thus, the heat exchanger does not seem to contribute to the oscillations. In addition, there is no significant dead time in the heat exchanger and a relatively long integral time (low I-action) , which makes it highly unlikely to be self-oscillating.

Further, it was believed that the control loop TIC-1402 which manipulates the air inlet valve was the sheer source of the oscillations in the system, as shown in figure 16. Figure 16 shows that there are some significant oscillations in the temperatures inside the catalyst bed and at the reactor outlet. It also shows the controller output which controls the air valve, which clearly contributes to the large variations in the temperatures in the reactor. The figure shows oscillations with a period of approximately 100 minutes. The controller signal shows that as the measured temperature rises above its setpoint, the controller provides an output. Due to the dead time throughout the catalyst bed, the controller TIC-1402 does not detect that the temperature inside the catalyst bed has dropped significantly at once, which makes the temperature undershoot. When the measured temperature is below the setpoint, the controller logically reaches saturation as the valve cannot have negative valve openings - i.e. the VOC content of the waste gas stream can only be decreased, not increased. Further, as the VOC concentration again increases, the temperature rises and the controller again provides an output after the dead time has passed.

Studying the behaviour of the process before the outlet temperature exceeds the setpoint and the air valve controller activates shows that some oscillations are present even before this happens. These variations are definitely most significant inside the reactor. This is an indication that the oscillatory behaviour of the reactor temperature may originate from periodic disturbances in the waste gas composition.

An analysis of the waste stream gas was obtained from Perstorp for one specific date. These are shown in appendix D. This strengthens the theory that upstream concentration variations might be the source of the problem. In addition, after quite a while, information about the upstream units which the catalytic incinerator treats waste gases from was retrieved which confirmed that these units were run batch-wise in approximately 100 minute periods. Hence, the plant data suggests that periodic variations in the VOC concentrations amplified by an overshooting air valve controller is the source of the large variations.

6 Control improvement

6.1 Simulation of current control structure

Before improving the existing control structure, the current plant behaviour was attempted reproduced in order to try to obtain the amplification of the disturbance using the air controller. The controllers were implemented in the simulink model for the total process shown in figure 9. The control structure in Simulink is shown in figure 17.

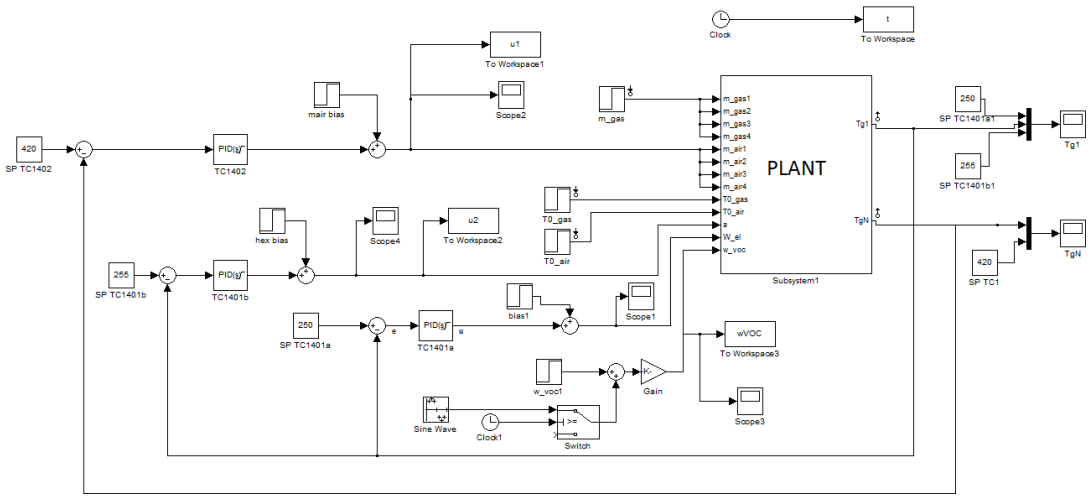

Figure 17: The control structure implemented in Simulink.

The electric heater isn't further focused on in this project, as it can be completely disregarded when it comes to the problematic behaviour of the process control system. The heat exchanger bypass controller isn't emphasized either, because as explained in the previous chapter, it doesn't seem to be part of the disturbance amplification.

The air valve controller is implemented as a pure P-controller, as including the I-part caused issues with integral windup which were not resolved using Simulink.

As the real disturbance isn't a true sinusoidal and thus the period can be interpreted in several ways, two main cases were simulated: one with a sinusoidal disturbance with a period of 100 minutes, and one with a period of 50 minutes. The disturbance had an amplitude of 0.03 wt% VOC and a bias of 0.9 wt%. A step in the disturbance bias from

	TIC-1401b	TIC-1402
K	-0.05	-0.07
τ_i [s]	1920	0

Table 4: Controller parameters used to reproduce the existing control structure. The proportional gain is not scaled.

0.9 wt% to 1.1 wt% was introduced at t = 600 min in order to force the measured outlet temperature above its setpoint.

The controller parameters used are shown in table 4. The simulation results are shown in figure 18.

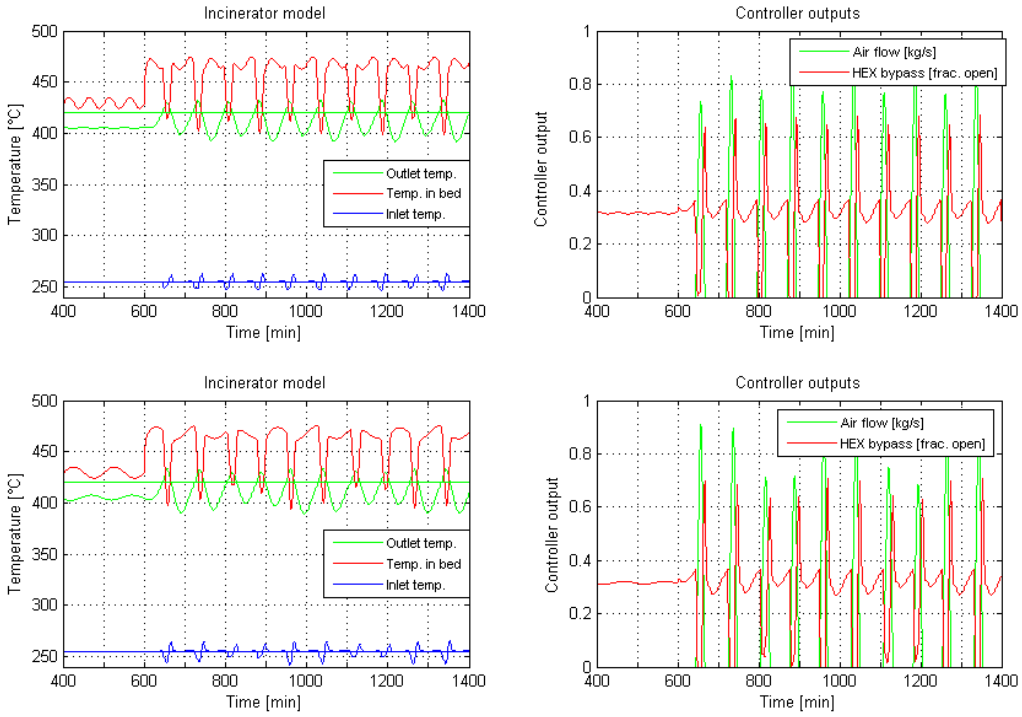

Figure 18: Simulation results using controller parameters in table 4. The disturbance has a period of 50 min in the top figures and 100 min in the bottom figures, and an amplitude of 0.03 wt% VOC and a bias of 0.9 wt%. A step in the bias from 0.9 wt% to 1.1 wt% is introduced at t = 600 min.

The behaviour of the plant obtained from this model is comparable with the one observed

K	-0.005
τ_I [s]	2400

Table 5: Controller parameters for TIC-1402 obtained by using the SIMC tuning rules. The proportional gain is not scaled.

in the real plant.

6.2 Control improvement

In this subchapter, two options for improving the dynamic control performance of the process will be investigated by simulation. These two options are control structures which use already existing sensors and actuators, and thus relatively easily can be implemented at the real plant.

6.2.1 Re-tuning of TIC-1402

The violent behaviour of TIC-1402 might simply be due to an overly agressive tuning. Hence, a re-tuning using the SIMC tuning rules was performed for the outlet temperature response for a step change in the air flow. This is shown in appendix A. The result is given in table 5. The corresponding simulation results are shown in figure 19.

Comparing figure 18 and 19 shows that the magnitude of the temperature variations in the catalytic incinerator is noticeably reduced. This indicates that the main source of the severe oscillations originates from a too high proportional gain for TIC-1402 at the real plant. Overly agressive tuning combined with a considerable dead time will always produce oscillations. Virtually, with such processes, one must always find an appropriate trade-off between response time and stability.

6.2.2 Cascade control

As mentioned in chapter 2.3.2, cascade control can be applied when the process dynamics are such that the secondary or inner-loop controller can detect and thus compensate for a disturbance significantly faster than the primary or outer-loop controller.

In this case, the plant data show that the temperature inside the catalyst bed has a significantly faster response than the outlet temperature, which is the controlled variable

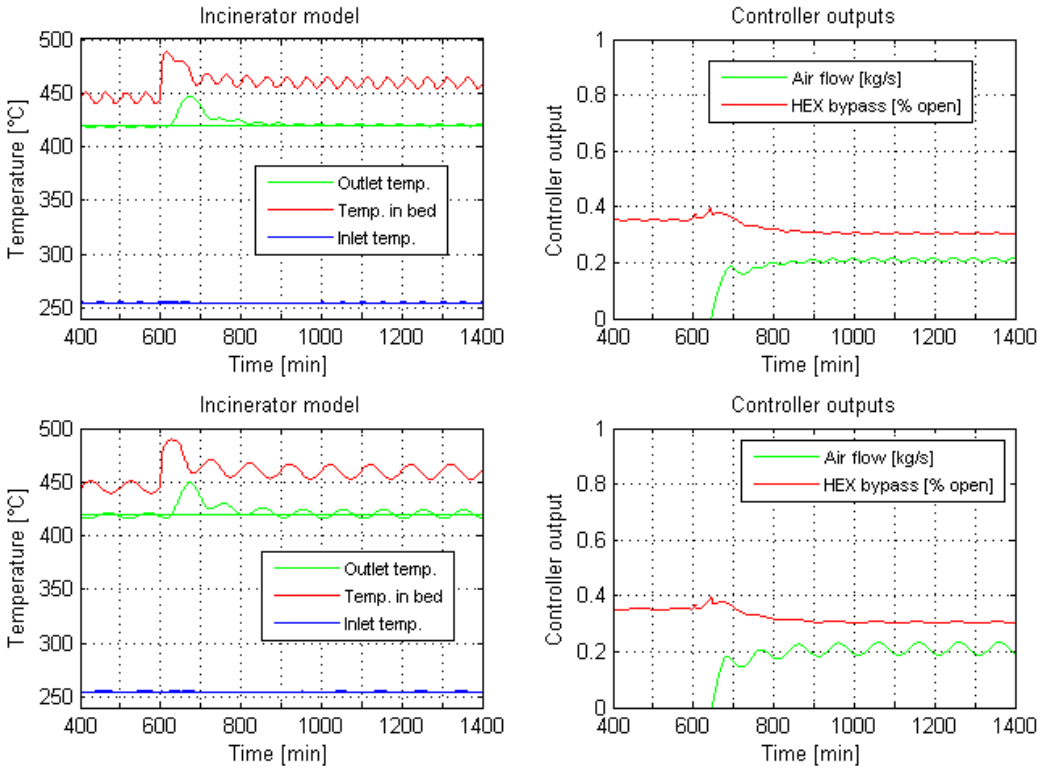

Figure 19: Simulation results using controller parameters in table 5. The disturbance has a period of 50 min in the top figures and 100 min in the bottom figures, and an amplitude of 0.03 wt% VOC and a bias of 0.98 wt%. A step in the bias from 0.98 wt% to 1.18 wt% is introduced at t = 600 min.

of TIC-1402. The setpoint of 420 C is given for the outlet temperature. There is no specification given for the temperature in the bed. However, using cascade control using the temperature in the bed as the controlled variable for the inner loop and the outlet temperature for the outer loop this will not be an issue, as the outer loop determines the setpoint for the inner.

First the inner loop was tuned using the SIMC rules for a step in the air flow. Secondly, the outer loop was tuned for a step in the setpoint of the inner loop. The SIMC rules were used for initial tuning, and then some manual tuning was needed in order to optimize the control. The responses and calculations are shown in appendix **??** and the results in table 6.

	Inner loop	Outer loop
K	-0.011	1.06
τ_I [s]	90	11520

Table 6: Controller parameters used for cascade control structure. The proportional gain is not scaled.

The results for a step change and sinusoidal disturbance corresponding to the one in chapter 6.2.1 at t = 600 min is shown in figure 20.

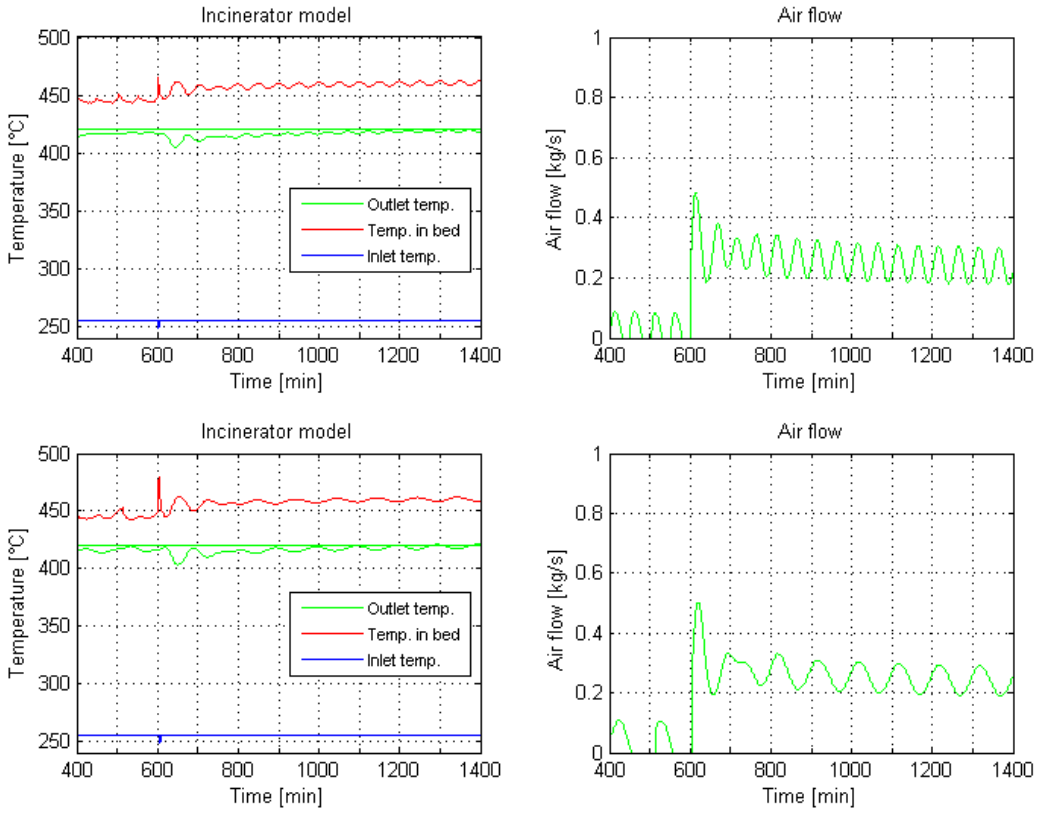

Figure 20: Simulation results using cascade control. The disturbance has a period of 50 min in the top figures and 100 min in the bottom figures, and an amplitude of 0.03 wt% VOC and a bias of 0.9 wt%. A step in the bias from 1.0 wt% to 1.2 wt% is introduced at t = 600 min.

As can clearly be seen from the figure, a disturbance using this cascade control scheme results in temperature variations of considerably lower magnitude than the control scheme

that is currently applied at the plant. It also seems to have a slight advantage over the re-tuned controller from the previous chapter.

7 Discussion

7.1 The model

7.1.1 General

In this project, most of the variables such as heat capacities, pressures etc. are treated as constants. For gases, this is not always reasonable to assume. However, from plant data it is shown that the pressures are close to atmospheric throughout the process. In addition, the change in heat capacity will only have a negligible effect on the dynamics. Thus, as this is a dynamic study, these simplifications were made.

For the heat exchanger, the shell and tube side heat transfer coefficients were treated as constants as well. By testing with different plant data for various flowrates, it was discovered that this is not a reasonable assumption. However, as it was relatively early in the thesis discovered that the heat exchanger was not the main problem for the control, this was disregarded.

The adjustment of the parameters shown in chapter 4 is also done more or less by trial and error, and were chosen as to best possible match the real data. However, as they all affect each other, it is not a trivial task. After spending an excessive amount of time on this, it was decided to not put too much emphasis on this as it actually doesn't affect the dynamics to a considerable degree.

The model does not include any dynamics for the valves, which may be an issue in practice.

7.1.2 The catalytic incinerator

The main problem encountered in this thesis was getting the correct dynamics for the temperatures throughout the reactor. A catalyst mass of 280 kg was provided by Perstorp, but using this value resulted in too fast dynamics. As the time constant throughout the bed is given both by the heat transfer between the gas and catalyst and the mass of the catalyst, a lot of trial and error was performed in order to try to slow down the dynamics. As the reaction was assumed to occur directly in the catalyst phase, the temperature peak in the catalyst bed increased dramatically when reducing the heat transfer to the gas phase. It is also shown in literature [6] that this such heat transfer is

of a large magnitude. As a last resort, it was decided to increase the mass of the catalyst bed in order to have a reasonable model to work with for the control improvement part of the project.

The reaction was modelled as an instantaneous occurence in the catalyst element in which the ignition temperature was exceeded. Whether or not this is a reasonable assumption is not completely clear, but catalytic combustion reactions, especially in the presence of excess oxygen, usually have high reaction rates. Nonetheless, towards the end of the project, implementing a kinetic model for the catalytic oxidation of MIBK was attempted, hoping that this would provide more correct dynamics. The model was based on the article *"The kinetic of the catalytic decomposition of methyl isobuthyl ketone over a Pt/γ-alumina catalyst"*. Sadly, due to insufficient time, this could not be completed. Including a kinetic model would also make the reaction rate dependent on the temperature due to Arrhenius' law, which might in turn increase the oscillations in the reactor further if the heat exchanger bypass controller isn't able to keep te inlet temperature to the reactor constant. Though, this effect is not possible to investigate using the model in this project.

As mentioned, the reaction is assumed to occur in the catalyst phase only. No mass transfer limitations are included in the model. Whether or not this is a pronounced effect in the real plant is not known, and should be further investigated.

7.2 The control aspect

Thorough examination of excessive amounts of plant data strengthens the theory that the periodic variations in the inlet compositions plus the overly agressive air valve controller combined with a significant dead time is the main source of the occasional huge variations at the plant. This was further verified by the simulations results in chapter 6, provided that the model actually exhibits the correct behaviour and input/disturbance correlations.

Reducing the proportional gain according to the SIMC tuning rules for PI controllers resulted in a significant reduction in the amplitude of the oscillations in the temperatures throughout the reactor, and thus a more stable performance. The SIMC tuning rules developed by Prof. Sigurd Skogestad never cease to impress. However, this does not compensate for the dead time in the process. Using pure PI-controllers for lag-dominant processes will always involve a certain trade-off between accuracy and response time.

As expected, cascade control provided the most optimal results with the best disturbance rejection as it is able to compensate for the disturbance before it is detected in the outlet temperature.

The pressure controller was decided not included in this work, in agreement with my supervisors at NTNU, as it was assumed not have a major impact on the dynamics. However, in an eventual further study, this should perhaps be further investigated.

8 Conclusion

By analyzing the dynamic data from the actual plant, it was discovered that the possible source of the ocassional large temperature variations in the incinerator is the periodic variations in the inlet compositions, plus the overly agressive air valve controller combined with a significant dead time. This results in oscillations due to overshooting. This behaviour was successfully reproduced using the derived model.

Two possibilities for improving the control performance were investigated, both using already existing sensors and actuators.

The first control improvement involved reducing the proportional gain according to the SIMC tuning rules for PI controllers. This resulted in a significant reduction in the amplitude of the oscillations in the temperatures throughout the reactor, and thus a more stable performance.

Finally, cascade control was implemented using the faster-responding catalyst bed temperature for the inner loop, and the reactor outlet temperature for the outer loop. This provided the most optimal results with the best disturbance rejection as it is able to compensate for the disturbance before it is detected in the outlet temperature.

8.1 Further work

As mentioned in the discussion chapter, a further study should look into the effects of implementing reaction kinetics and mass transfer resistances. Also, the pressure controller might be of interest.

References

[1] Myke King. *Process Control - A Practical Approach*. John Wiley and Sons Ltd, West Sussex, UK, 2011.

[2] Sigurd Skogestad. Simple analytic rules for model reduction and pid controller tuning. *Journal of Process Control*, 13, 2003.

[3] Sigurd Skogestad and Ian Postlethwaite. *Multivariable Feedback Control - Analysis and Design*. John Wiley and Sons Ltd, West Sussex, UK, 1996.

[4] Knut Wiig Mathisen. *Integrated Design and Control of Heat Exchanger Networks*. PhD thesis, University of Trondheim, 1994.

[5] MathWorks Inc. Documentation center: What is an s-function? http://www.mathworks.se/help/simulink/sfg/what-is-an-s-function.html. Accessed: 12/2012.

[6] Gilbert G. Froment and Kenneth B. Bischoff. *Chemical Reactor Analysis and Design*. John Wiley and Sons Ltd, 1979.

A SIMC re-tuning of TIC-1402

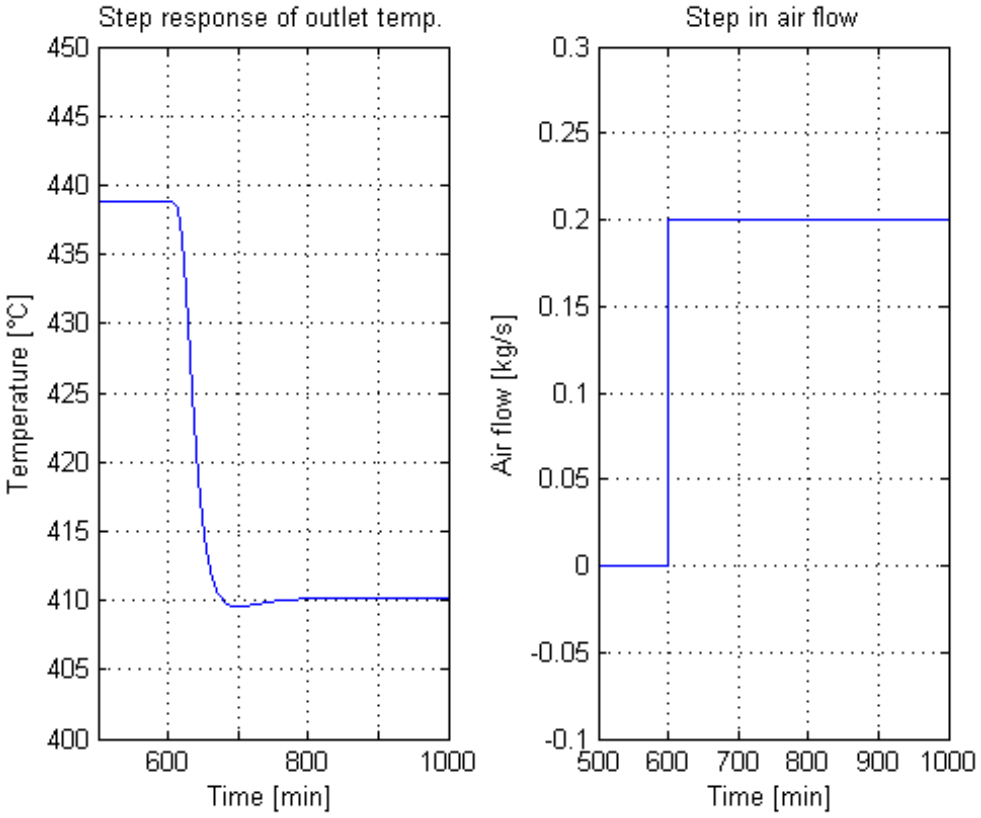

Figure A.1: Step response of outlet temperature for re-tuning of TIC-1402.

Using the SIMC rules as explained in chapter 2.2.4.

$$k = \frac{\Delta y}{\Delta u} = \frac{(410 - 439)}{(0.2 - 0)} = -145 \tau_1 = 40min = 2400s \theta = 14min = 840s \tag{A.1}$$

Choosing $\tau_c = \tau_1$ yields

$$\tau_I = min\{\tau_1, 4(\tau_c + \theta)\} = 2400s K_c = \frac{1}{k} \frac{\tau_I}{\tau_c + \theta} = -0.005 \tag{A.2}$$

B Cascade controller tunings

B.1 Inner loop

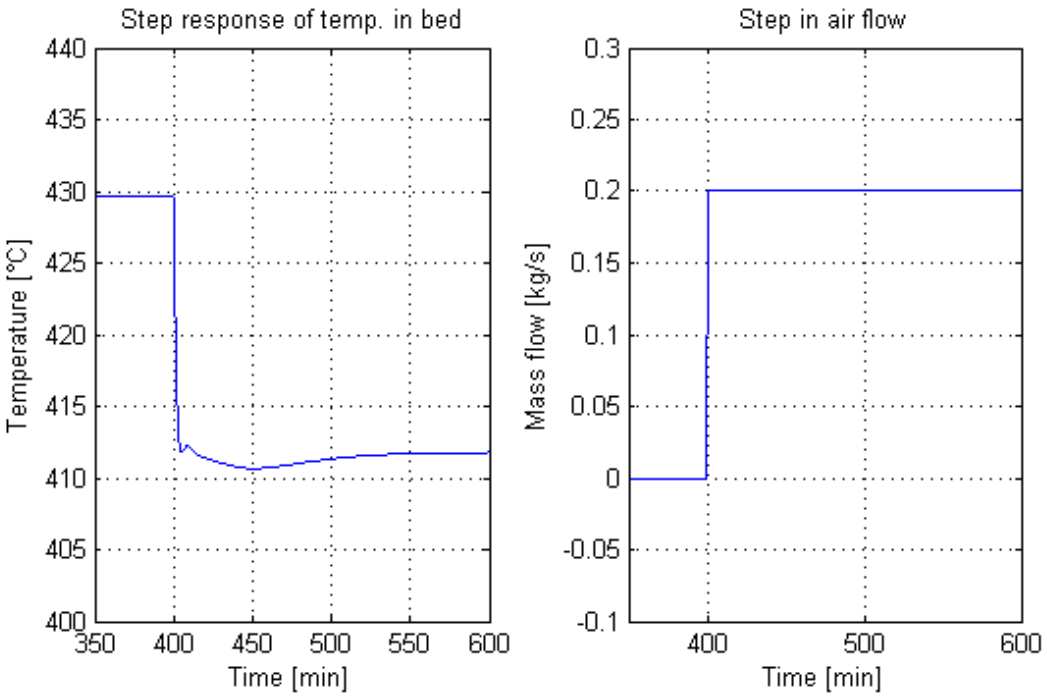

Figure B.1: Step response of temperature in catalyst bed used for tuning of the inner loop of the cascade controller.

Using the SIMC rules as explained in chapter 2.2.4.

$\theta = 0$

Choosing $\tau_c = \tau_1$ yields

$$\tau_I = min\{\tau_1, 4(\tau_c + \theta)\} = 90sK_c = \frac{1}{k}\frac{\tau_I}{\tau_c + \theta} = -0.011 \tag{B.1}$$

B.2 Outer loop

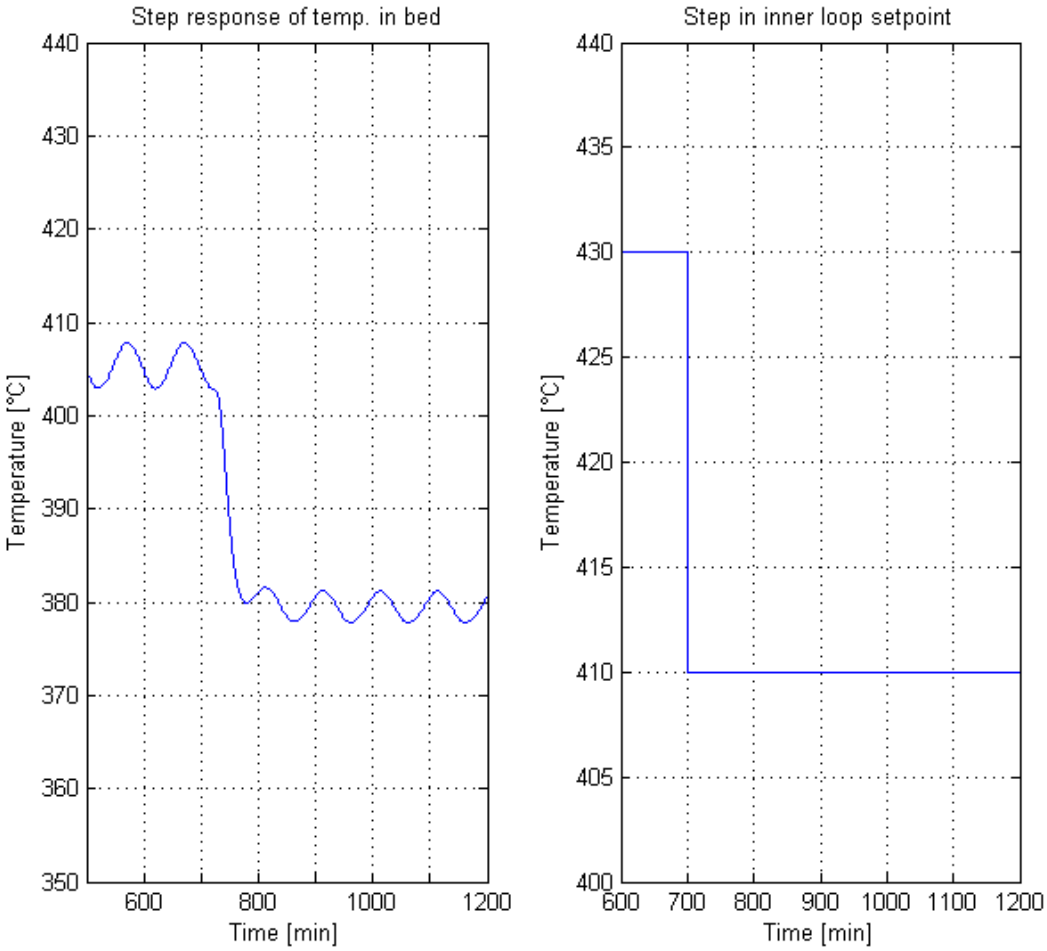

Figure B.2: Step response of temperature in reactor outlet used for tuning of the outer loop of the cascade controller.

$$k = \frac{(380 - 405)}{(410 - 430)} = 1.25\tau_1 = 48min = 2880s\theta = 25min = 1500s \tag{B.2}$$

Choosing $\tau_c = \tau_1$ yields

$$\tau_I = 2880sK_c = 0.53 \tag{B.3}$$

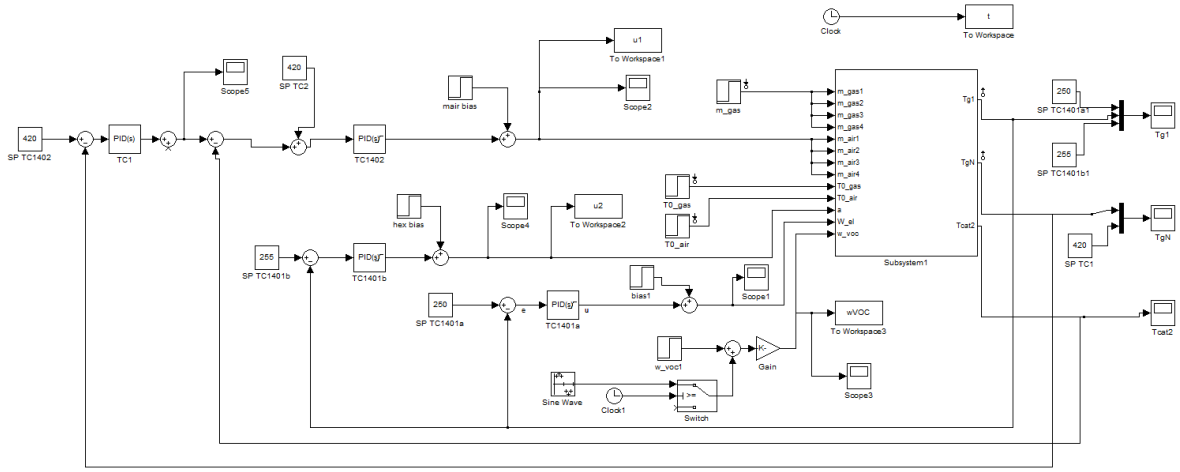

Figure B.3: The cascade structure in Simulink

C P&ID of process

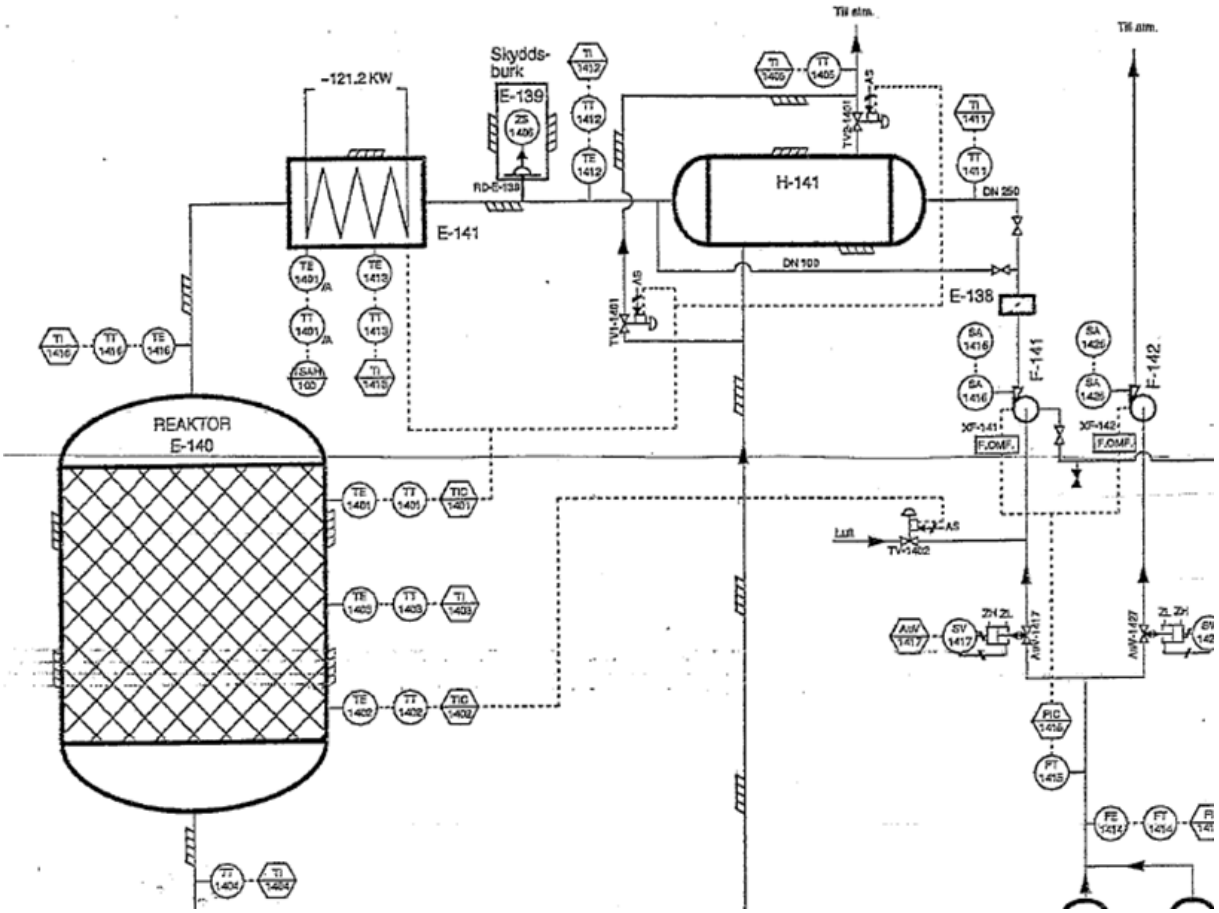

Figure C.1: P&ID of process.

D Gas composition variations

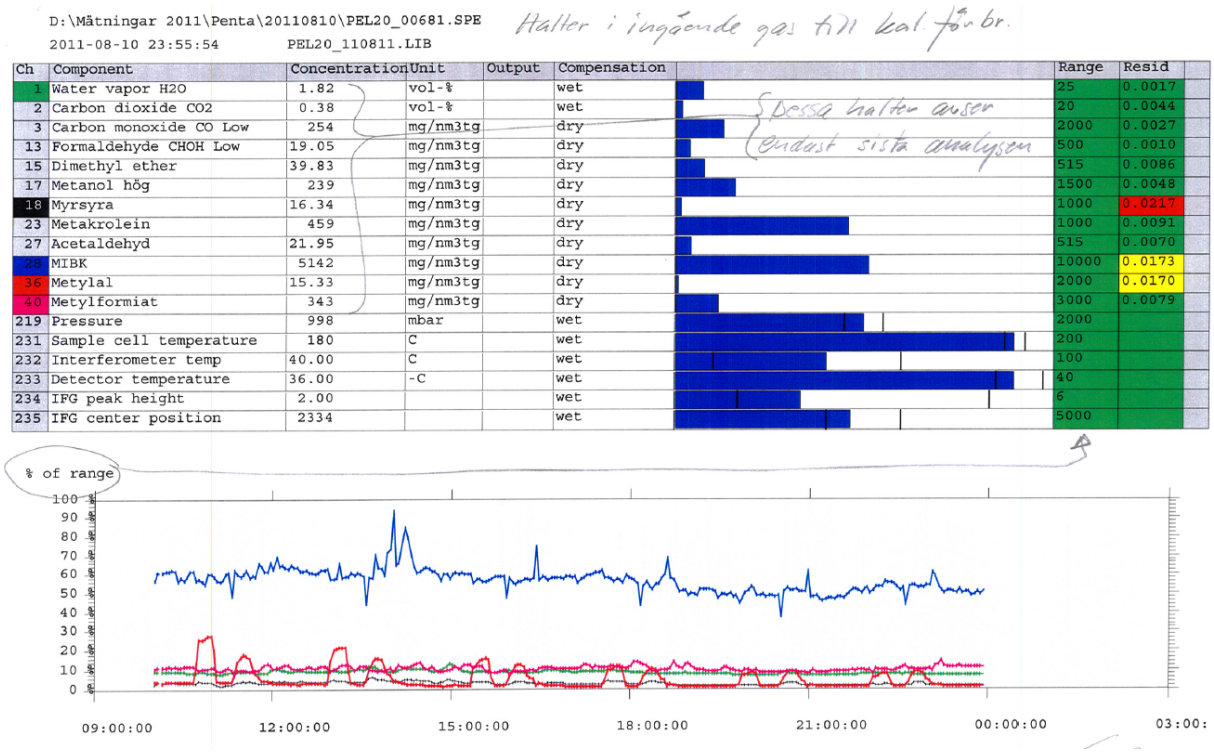

Ch	Component	Concentration	Unit	Output	Compensation	Range	Resid
1	Water vapor H2O	1.82	vol-%		wet	25	0.0017
2	Carbon dioxide CO2	0.38	vol-%		wet	20	0.0044
3	Carbon monoxide CO Low	254	mg/nm3tg		dry	2000	0.0027
13	Formaldehyde CHOH Low	19.05	mg/nm3tg		dry	500	0.0010
15	Dimethyl ether	39.83	mg/nm3tg		dry	515	0.0086
17	Metanol hög	239	mg/nm3tg		dry	1500	0.0048
18	Myrsyra	16.34	mg/nm3tg		dry	1000	0.0217
23	Metakrolein	459	mg/nm3tg		dry	1000	0.0091
27	Acetaldehyd	21.95	mg/nm3tg		dry	515	0.0070
28	MIBK	5142	mg/nm3tg		dry	10000	0.0173
36	Metylal	15.33	mg/nm3tg		dry	2000	0.0170
40	Metylformiat	343	mg/nm3tg		dry	3000	0.0079
219	Pressure	998	mbar		wet	2000	
231	Sample cell temperature	180	C		wet	200	
232	Interferometer temp	40.00	C		wet	100	
233	Detector temperature	36.00	-C		wet	40	
234	IFG peak height	2.00			wet	6	
235	IFG center position	2334			wet	5000	

Figure D.1: Typical input concentration variations.

E Some examples of the Matlab code

E.1 Parameters

```
%%%%%%%%%%%%%%%%%%%%%%%%%%%%%%%%%%%%%%%%%%%%%%%%%%%%%%%%%%%%%%%%%%%%%%%%
%%%%%%%   Process parameters and values  %%%%%%%%%%
%%%%%%%%%%%%%%%%%%%%%%%%%%%%%%%%%%%%%%%%%%%%%%%%%%%%%%%%%%%%%%%%%%%%%%%%


global par

%%%%%%%%%%%%%%%%%% General %%%%%%%%%%%%%%%%%%%%%%%%%

par.P           = 1;                % Process pressure [atm]
par.M           = 0.029;            % Molar mass of gas (air) [kg/mol]
par.R           = 8.2057*10^-5;     % Universal gas constant %[m^3atm/Kmol]

%%%%%%%%%%%%%%%%%% Pipes %%%%%%%%%%%%%%%%%%%%%%%%%%%

par.dypipe      = 0.3239;
par.dpipe       = 0.008;



%%%%%%%%%%%%%%%%% Air feed %%%%%%%%%%%%%%%%%%%%%%%%%%

par.Vmix        = 1;                % Volume where fed air and process gas is mixed [m^3]

%%%%%%%%%%%%%%%%%% Heat exchanger %%%%%%%%%%%%%%%%%%%

par.Nhex        = 10;               % Number of "mixing tanks"

% ----- Adjusted parameters -----
par.hh          = 40;%35;               % Hot side heat transfer coefficient [W/m^2C]
par.hc          = par.hh;               % Cold side heat transfer coefficient [W/m^2C]
% ---------------------------------

par.cph         = 1100;             % Hot side gas heat capacity [J/kgC]
par.cpc         = 1030;             % Cold side gas heat capacity [J/kgC]
par.cpw         = 500;              % HEX wall heat capacity [J/kgC]
```

```
par.A           = 115;                      % Total heat transfer area [m^2]
par.Ah          = par.A/par.Nhex;           % Heat transfer area hot side [m^2]
par.Ac          = par.A/par.Nhex;           % Heat transfer area cold side [m^2]
par.Aw          = par.A/par.Nhex;           % Area of one wall segment [m^2]

par.Vh_tot      = 2.3;                      % Hot side volume of HEX provided by Perstorp [m^3]
par.Vc_tot      = 1.8;                      % Cold side volume of HEX provided by Perstorp [m^3]
par.Vh          = par.Vh_tot/par.Nhex;      % Hot side volume of one HEX element [m^3]
par.Vc          = par.Vc_tot/par.Nhex;      % Cold side volume of one HEX element [m^3]

par.mhex        = 1300;                     % Mass of HEX provided by Perstorp [kg]
par.mw          = par.mhex/par.Nhex;        % Mass of one wall element [kg]

par.wH2O        = 0.020;%0.008;             % mass fraction H2O
par.Hvap        = 2257000;                  % Heat of vap. [J/kg]

%%%%%%%%%%%%%%%  Electric heater  %%%%%%%%%%%%%%%%%%%%%%%%%%%%%%%%

par.Velh        = 0.25;             % Volume of electric heater [m^3]


par.cpg         = 1030;             % Gas heat capacity [J/kgC]


%%%%%%%%%%%%%%%% Catalytic incinerator %%%%%%%%%%%%%%%%%%%%%%%%%%%%%

par.N           = 20;

% ----- Adjusted parameters -----
par.UAcat       = 10000*4;  % Heat transfer coefficient times area gas to catalyst [W/C]
par.kAcat       = 30;     % Heat conduction coefficient times cross-sectional area for catalyst [W
par.Vg          = 2.5;        % Gas volume inside incinerator [m^3]


% ---------------------------------


par.cpcat       = 1100;             % Heat capacity of catalyst (alumina) [J/kgC]
par.cpgas       = 1030;             % Heat capacity of gas [J/kgC]



par.mcat        = 280*5;              % Total mass of catalyst in incinerator, provided by Persto

par.deltaHc     = 35000000;         % Heat of combustion for organics (MIBK) [J/kg]
```

```
%%%%%%%%%%%%%%%%  Time delays  %%%%%%%%%%%%%%%%%%%%%%%%%%%%%%%%

f=1;

td1=1*f;
td2=0.5*f;
td3=0.2*f;
td4=0.3*f;
tdHEX=1*f;
tdel=0.3*f;
tdincin=3*f;



Lp1=5;
Lp2=2;
Lp3=4;
```

E.2 Heat exchanger model

```
function Tprime=HEX(t,X,U)

% The function is called by the s-function HEXs.m and calculates the
% derivatives of the temperatures in the hot side, cold side and wall
% elements, plus the hot side outlet temperature after bypass
% in a countercurrent gas-gas heat exchanger.

% The parameters are given in "parameters.m".

global par

%  Collecting parameters

%%
Nhex    =   par.Nhex;
hh      =   par.hh;
```

```
hc      =   par.hc;
cph     =   par.cph;
cpc     =   par.cpc;
cpw     =   par.cpw;
mw      =   par.mw;
Vh      =   par.Vh;
Vc      =   par.Vc;
Ah      =   par.Ah;
Ac      =   par.Ac;
Aw      =   par.Aw;
P       =   par.P;
R       =   par.R;
M       =   par.M;
Hvap    =   par.Hvap;



%%

% Splitting the states
Th      =   X(1:Nhex);                          % Gas temperatures in elements 1 to Nhex in hot si
Tc      =   X(Nhex+1:2*Nhex);                   % Gas temperatures in elements 1 to Nhex in cold s
Tw      =   X(2*Nhex+1:3*Nhex);                 % Wall temperature in elements 1 to Nhex
Thout   =   X(3*Nhex+1);                        % Hot outlet temperature after mixing bypass and h

% Inputs and disturbances
Tc0         = U(1);                             % Inlet temperature cold side
[C]
Th0         = U(2);                             % Inlet temperature hot side (outlet from reactor)
m           = U(3);                             % Mass flow of gas [kg/s]
mair        = U(4);                             % Mass flow of air fed to process [kg/s]
a           = U(5);                             % Hot side bypass fraction (a=0 -> no bypass)

% Defining length of output vectors
dThdt       =   zeros(Nhex,1);
dTcdt       =   zeros(Nhex,1);
dTwdt       =   zeros(Nhex,1);
dThoutdt    =   zeros(1,1);

if Th0 < 100
    wH2O    =   0;
elseif a == 1
    wH2O    =   0;
else
```

```
    wH2O    =   par.wH2O;
end


%%%%%%%%%%%%%%%   Calculation of state derivatives   %%%%%%%%%%%%%%%%%%%%%%


% ------------------------------ Initial elements ------------------------------

    dTcdt(1) =      (Tc0-Tc(1))*(((m+mair)*R*(Tc(1)+273.15))/(P*M*Vc)) ...
                    - (Tc(1)-Tw(Nhex))*(hc*Ac*R*(Tc(1)+273.15)/(cpc*P*M*Vc));

    dThdt(1) =      (Th0-Th(1))*(((m+mair)*(1-a)*R*(Th(1)+273.15))/(P*M*Vh))...
                    - (Th(1)-Tw(1))*(hh*Ah*R*(Th(1)+273.15)/(cph*P*M*Vh));


    dTwdt(1) =      ((Th(1)-Tw(1))*Ah*hh  +  (Tc(Nhex)-Tw(1))*Ac*hc)/(mw*cpw);


% ------------------------------ Remaining elements ------------------------------

for i=2:Nhex


    dTcdt(i) =      (Tc(i-1)-Tc(i))*(((m+mair)*R*(Tc(i)+273.15))/(P*M*Vc))...
                   -  (Tc(i)-Tw(Nhex+1-i))*(hc*Ac*R*(Tc(i)+273.15)/(cpc*P*M*Vc));


    dTwdt(i) =       ((Th(i)-Tw(i))*Ah*hh  +  (Tc(Nhex+1-i)-Tw(i))*Ac*hc)/(mw*cpw);

end

for i=2:Nhex-1

        dThdt(i) =      (Th(i-1)-Th(i))*(((m+mair)*(1-a)*R*(Th(i)+273.15))/(P*M*Vh))...
                    - (Th(i)-Tw(i))*(hh*Ah*R*(Th(i)+273.15)/(cph*P*M*Vh));
end

dThdt(Nhex) =   (Th(Nhex-1)-Th(Nhex))*(((m+mair)*(1-a)*R*(Th(Nhex)+273.15))/(P*M*Vh))...
                    - (Th(Nhex)-Tw(Nhex))*(hh*Ah*R*(Th(Nhex)+273.15)/(cph*P*M*Vh)) - (wH2O*
% - Hot outlet temperature after mixing bypass and heat exchanged stream -
```

```
    dThoutdt = ((m+mair)*a*Th0  + (m+mair)*(1-a)*Th(Nhex) - (m+mair)*Thout)*((R*(Thout+273.15))/(P

% Defines output vector

    Tprime=[dThdt; dTcdt; dTwdt; dThoutdt];

end
```

E.3 Heat exchanger s-function

```
function [sys,x0] = HEXs(t,x,u,flag)

%  Simulink interface to HEX.m
%
% Inputs:    t    - time in [s].
%            X    - States. A total of 3*N states.
%                   Temperatures of cold side gas, hot side gas and heat
%                   exchanger wall elements
%            U(1) - Inlet temperature hot side, Tc0 [C]
%            U(2) - Inlet hot gas temperature, Th0 [C]
%            U(3) - Mass flow of gas, m [kg/s]
%            U(4) - Mass flow of air fed to process, mair [kg/s]
%            U(5) - Hot side bypass fraction ( a=0 -> no bypass), a

% Outputs:   sys and x0 as described in the SIMULINK manual.
%            when flag is 0 sys contains sizes and x0 contains
%            initial condition.
%            when flag is 1, sys contains the derivatives,
%            and when flag is 3 sys contains outputs;
%            y(1:N)     - Gas temperatures in elements 1-N,hot side [C]
%            y(N+1:2N)  - Gas temperatures in elements 1-N, cold side [C]
%            y(2N+1:3N) - Wall temperatures in elements 1-N [C]
%            y(3N+1)    - Hot gas outlet temp. after bypass [C]

global  T0HEX par

if abs(flag) == 1
  % Return state derivatives.
  sys = HEX(t,x,u);

elseif abs(flag) == 3
```

```
  % Return system outputs.
  N = par.Nhex;
  sys(1,1:3*N+1) = x(1:3*N+1);

elseif flag == 0
  % Ininitalize the system
 % ssvaluesinit
  parameters
  x0 = T0HEX;
  N = par.Nhex;
  sys = [3*N+1, 0, 3*N+1, 5, 0, 0];

else
  sys = [];

end
```

E.4 Incinerator model

```
function dTdt=incin(t,X,U)

% This function is called by the s-function incins.m and calculates the
% derivative of the temperature of the gas leaving the electric heater.

%            X(1:N)    - Gas temperature in element 1 to N [C]
%            X(N+1:2*N)- Catalyst temperature in element 1 to N [C]

% The parameters are given in "parameters.m".

global par

% Collecting parameters

%%
N           =   par.N;
cpcat       =   par.cpcat ;
cpgas       =   par.cpgas;
UAcat       =   par.UAcat;
%UAcatinf    =   par.UAcatinf;
UAwall      =   par.UAwall;
kAcat       =   par.kAcat;
Tamb        =   par.Tamb;
```

```
mcat        =   par.mcat;
deltaHc     =   par.deltaHc;
Vg          =   par.Vg;
P       =   par.P;
R       =   par.R;
M       =   par.M;
%MwMIBK  = par.MwMIBK;

%%


% Defining the states
T = X(1:2*N)';                              % X(1:N) - Gas temperature in element 1-N [C]
                                            % X(N+1:2*N)- Catalyst temperature in element 1-N [C]


% Inputs and disturbances
T0      = U(1);                             % Inlet temperature to incinerator [C]
m       = U(2);                             % Mass flow of process gas [kg/s]
mair    = U(3);                             % Mass flow of air fed to process [kg/s]
w       = U(4);                             % Mass fraction of VOC

beta=1;



%%%%%%%%%%%%%%   Calculation of state derivatives   %%%%%%%%%%%%%%%%%%%%%%

% ------------------------------  Initial elements ----------------------------------


% Gas phase
dTdt(1)=    (((N*(m+mair)*R*(T(1)+273.15))/(P*M*Vg))*(T0-T(1)))...
            -((UAcat*R*(T(1)+273.15)/(P*M*Vg*cpgas))*(T(1)-(T(N+1))));

% Catalyst phase
dTdt(N+1)=  (UAcat/(mcat*cpcat)*(T(1)-T(N+1)))...
            +((kAcat*N/(mcat*cpcat))*(T(N+2)-T(N+1))) -(UAwall/(mcat*cpcat))*(T(N+1)-(Tamb));

% ------------------------------ Interior elements ----------------------------------
% Gas phase
for i=2
```

```
                        %UAcat=par.UAcatinf;

            dTdt(i)=    (((N*(m+mair)*R*(T(i)+273.15))/(P*M*Vg))*(T(i-1)-T(i)))...
                        -((UAcat*R*(T(i)+273.15)/(P*M*Vg*cpgas))*(T(i)-(T(N+i))))+(1-beta)*
% Catalyst phase


            dTdt(N+i)=  (UAcat/(mcat*cpcat)*(T(i)-T(N+i))) + (kAcat*N*N/(mcat*cpcat))*(T(N+
                        w=0; % Sets mass fraction of VOC to 0 after combustion
                        %UAcat=par.UAcat;
  for i=3:(N-1)
                   % Below ignition temperature
             dTdt(i)=    (((N*(m+mair)*R*(T(i)+273.15))/(P*M*Vg))*(T(i-1)-T(i)))...
                         -((UAcat*R*(T(i)+273.15)/(P*M*Vg*cpgas))*(T(i)-(T(N+i))));
            dTdt(N+i)=  (UAcat/(mcat*cpcat)*(T(i)-T(N+i))) + (kAcat*N*N/(mcat*cpcat))*(T(N+
                        -(UAwall/(mcat*cpcat))*(T(N+i)-(Tamb));
        end


                        %%%%%%%%%%%%%%%%%%%%%%%%%%%%%%%%%%%%%%%%%%%%%%%%%%%%%%%%%%%%%%%%%%%
        end




%------------------------------ Final elements ------------------------------
% Gas phase
     dTdt(N)=     (((N*(m+mair)*R*(T(N)+273.15))/(P*M*Vg))*(T(N-1)-T(N)))...
                  -((UAcat*R*(T(N)+273.15)/(P*M*Vg*cpgas))*(T(N)-T(2*N)));
%Catalyst phase
     dTdt(2*N)=   (UAcat/(mcat*cpcat)*(T(N)-T(2*N)))    +((kAcat*N/(mcat*cpcat))*(T((2*N)-1)-
                  -(UAwall/(mcat*cpcat))*(T(2*N)-(Tamb));   % Catalyst


 % Defining output vector

 dTdt = [dTdt];
```